D5.1: Climate Assessment Report (CAR)

Reference: CCI_LAKES2-0034-CAR

Issue 2.0.2.2

11 rue Hermès, Parc Technologique du Canal — 31520 Ramonville Saint-Agne, France
Tel +33 (0)5 61 39 47 00 Fax +33(0)5 61 75 10 14
www.cls.fr

CHRONOLOGY ISSUES

Issue/	Date	Objective	Written by
2.0.2.0	15/11/2023	Draft	Pinardi M., Giardino C., Caroni R., Amadori M., Tellina G., Bresciani M. (CNR) Jiang D., Spyrakos E., Jones I. (UoS) Scholze J., Stelzer K. (BC)
2.0.2.1	15/12/2023	Internal review	S.Simis
2.0.2.2	31/01/2024	Reviewed by ESA	Pinardi M

Note: the versioning of the CAR will now follow the version of CRDP that is described. In this document the version v2.0.2 of the CRDP is analyzed.

Checked by	Stefan Simis - PML	Stefan Simis 05/02/2024
Approved by	Alice Andral - CLS	A.Andral 05/02/2024
Authorized by	Clément Albergel - ESA	Clement Albergel 05/02/2024

DISTRIBUTION

Company	Names	Email
ESA	Clément Albergel	clement.albergel@esa.int
BC	Carsten Brockman	carsten.brockmann@brockmann-consult.de
BC	Dagmar Müller	dagmar.mueller@brockmann-consult.de
BC	Jorrit Scholze	jorrit.scholze@brockmann-consult.de
BC	Kerstin Stelzer	kerstin.stelzer@brockmann-consult.de
BC	Martin Boettcher	martin.boettcher@brockmann-consult.de
BC	Olaf Danne	olaf.danne@brockmann-consult.de
CLS	Alice Andral	aandral@groupcls.com

CLS	Anna Mangilli	amangilli@groupcls.com
CLS	Beatriz Calmettes	bcalmettes@groupcls.com
CLS	Nicolas Taburet	ntaburet@groupcls.com
CLS	Christophe Fatras	cfatras@groupcls.com
CLS	Pierre Thibault	pthibaut@groupcls.com
CNR	Claudia Giardino	giardino.c@irea.cnr.it
CNR	Mariano Bresciani	bresciani.m@irea.cnr.it
CNR	Monica Pinardi	pinardi.m@irea.cnr.it
CNR	Marina Amadori	amadori.m@irea.cnr.it
CNR	Rossana Caroni	caroni.r@irea.cnr.it
CNR	Giulio Tellina	tellina.g@irea.cnr.it
H2O Geo	Claude Duguay	claude.duguay@h2ogeomatics.com
H2O Geo	Yuhao Wu	mark.wu@h2ogeomatics.com
H2O Geo	Jaya Sree Mugunthan	jayasree.mugunthan@h2ogeomatics.com
H2O Geo	Justin Murfitt	justin.murfitt@h2ogeomatics.com
HYGEOS	François Steinmetz	fs@hygeos.com
LEGOS	Jean-François Cretaux	jean-francois.cretaux@cnes.fr
LEGOS	Paul-Gérard Gbektom	paul.gerard.gbetkom@legos.obs-mip.fr
PML	Stefan Simis	stsi@pml.ac.uk
PML	Xiaohan Liu	liux@pml.ac.uk
PML	Nick Selmes	nse@pml.ac.uk
PML	Mark Warren	mark1@pml.ac.uk
Sertit	Hervé Yésou	Herve.yesou@unistra.fr
Sertit	Jérôme Maxant	maxant@unistra.fr
Sertit	Sabrina Amsil	s.amzil@unistra.fr
Sertit	Rémi Braun	remi.braun@unistra.fr
UoR	Chris Merchant	c.j.merchant@reading.ac.uk
Bangor	Iestyn Woolway	iestyn.woolway@bangor.ac.uk
UoR	Laura Carrea	l.carrea@reading.ac.uk
UoS	Dalin Jiang	dalin.jiang@stir.ac.uk
UoS	Evangelos Spyrakos	evangelos.spyrakos@stir.ac.uk
UoS	Ian Jones	ian.jones@stir.ac.uk

LIST OF CONTENTS

1 Executive summary 7
2 Introduction 9
2.1 Purpose of this document 9
2.2 Structure of the document 9
3 Products of the Lakes_cci 10
4 Data exploration 11
4.1 The Lakes_cci data at a glance 11
4.1.1 Spatial distribution 11
4.1.2 Global distribution of ECVs 12
5 Local-scale assessment 17
5.1 Lake Garda (Italy) 17
5.1.1 Satellite-based evaporation mapping 17
5.1.2 Spatio-temporal bio-geophysical surface features 20
6 Regional-scale assessment 23
6.1 South American lakes 23
7 Global scale assessment 31
7.1 Trends of water quality in shallow lakes 31
7.2 Meteorological factors influencing LSWT across different climates 33
8 Use cases 37
8.1 Heatwave and storm event impacts on lakes (CNR) 37
8.2 La Niña influence on water quantity and quality of a reservoir in a hot desert climate (Lake Qadisiyah, Iraq) (UoS) 40
8.3 Aggregated climate indicators for the global lakes dataset (BC) 44
8.3.1 Lakes_cci climate indicators 45
8.3.2 Visualisation of climate indicators 47
8.3.3 Examples 48
9 Progress on user requirements 50
9.1 Updates on user requirements 50
10 External studies 55
11 Conclusions 56
12 References 57

LIST OF TABLES AND FIGURES

Table 2. Lake name, type, area, average depth, trophic status, ecosystem services and main uses for the subset of South American lakes investigated. The reference reported are listed as footnotes. 24

Table 3. Summary of target GCOS requirements for the Lakes ECV ("2-sigma"). Thematic ECVs are Lake Water Level (LWL), Lake Water Extent (LWE), Lake Surface Water Temperature (LSWT), Lake Ice Cover (LIC), Lake Ice Thickness (LIT), Lake Water Leaving Reflectance (LWLR). 50
Table 4. Summary of threshold and target of GCOS requirements for the lake water level (LWL) variable, current status about the achievement of the requirements. 51
Table 5. Summary of threshold and target of GCOS requirements for the lake surface water temperature (LSWT) variable, current status about the achievement of the requirements. 51
Table 6. Summary of threshold and target of GCOS requirements for the lake water extent (LWE) variable, current status about the achievement of the requirements. 52
Table 7. Summary of threshold and target of GCOS requirements for the lake ice cover (LIC) variable, current status about the achievement of the requirements. 52
Table 8. Summary of threshold and target of GCOS requirements for the lake ice thickness (LIT) variable, current status about the achievement of the requirements. 53
Table 9. Summary of threshold and target of GCOS requirements for the lake water leaving reflectance-(LWLR) variable, current status about the achievement of the requirements. 53

Figure 1. Global distribution of the Lakes_cci dataset (v2.0.2). 12
Figure 2. Distribution of Chl-a concentration, annual average calculated per lake, for CRDP v1.1 from 2002 to 2019 (left) and for v2.0.2 from 2002 to 2020 (right). Some outlier values of Chl-a have been removed for clarity. 13
Figure 3. Lake trophic status classification based on the average Chl-a concentration (mg m^{-3}) for the global dataset (V2) from 2016 to 2020. In the pie chart the number of lakes per category is reported. 14
Figure 4. Distribution of turbidity (NTU), annual average calculated per lake, for the global dataset V1.1 from 2002 to 2019 (left) and for dataset 2.0.2 from 2002 to 2020 (right). Some outliers were removed for clarity. 14
Figure 5. Distribution of lake surface water temperature (LSWT; °C). Annual averages calculated per lake, for (left) CRDP v1.1 from 2002 to 2019 and (right) CRDP v2.0.2 from 2002 to 2020. Note that bimodal distributions are derived from lakes being either closer to temperate or equatorial regions. 15
Figure 6. Distribution of normalised (%) lake level, calculated per lake (left) and reservoir (right) typology as annual average divided by time-series average, for the global dataset. Scaled between 96-104% for clarity. 16
Figure 7. Workflow for the generation of evaporation products from LSWT maps. Left: Schematic of the terms of the heat balance in a water body and data sources. Right: example of maps of instantaneous evaporation in mm/h and time series of spatially averaged daily evaporation in mm/d. Figure modified from Matta et al. (2022). 18
Figure 8. Top: hourly evaporation from Lake Garda estimated with the LakeVap tool in year 2017 fed by Lakes_cci LSWT maps and ERA5 meteorological data. Bottom: daily evaporation from Lake Garda (spatial average from daily evaporation maps). The gaps in the time series highlight when LSWT maps are not available for more than 60 consecutive days. Figure modified from Matta et al. (2022). 20
Figure 9. First dominant mode (EOF1) from LSWT (a), Chl-a (b) and turbidity (c) from Empirical Orthogonal Function analysis on anomalies. 21
Figure 10. (a) autocorrelation functions of LSWT anomalies in each pixel of the maps (grey lines), of the spatial mean of LSWT anomaly (thick grey line) and corresponding exponential fitting (red line). (b) map of MLD estimated with Hasselman's theory; (c) bathymetry; (d-f) thermal profiles from three in situ observations (black dots in (d) map). 22
Figure 11. List and map of distribution of the 10 selected lakes in South America. Latitude in italics in the table refer to lakes at latitude <-23.5 used as threshold for LSWT trend analysis. 24
Figure 12. South American lakes with (left) depth, trophic status, residence time and area information and (right) results from the Theil-Sen analysis with deseasonalised trends in Chl-a, turbidity, LSWT, and weather (air temperature (t2m) and total precipitation (tp)). 27

Figure 13. Map of results from the Theil-Sen analysis with deseasonal (DS) and seasonal trends in chlorophyll-a (left), Turbidity (centre) and lakes surface water temperature (LSWT; right) in the 10 South American selected lakes. MAM=March-April-May; JJA=June-July-August; SON=September-October-November; DJF=December-January-February. For LSWT the trend is reported for DJF at latitudes < -23.5 and deseasonalised for the (sub)tropical region. 28
Figure 14.Lake surface water temperature (LSWT) anomaly indicator (left) and Heatwave occurrence indicator (right) for the Lake Musters, Lake Buenos Aires, and Viedma Lake. 29
Figure 15. Lake surface water temperature (LSWT) anomaly indicator (left) and Heatwave occurrence indicator (right) for the Cerros Colorado Complex and Villarrica Lake. 30
Figure 16. Lake surface water temperature (LSWT) anomaly indicator (left) and Heatwave occurrence indicator (right) for Lake Titicaca, Mirim Lagoon and Castillos Lagoon. 30
Figure 17. Map of distribution for Chl-a trends (orange=positive trend; blue=negative trend; overlaying star=significant trend) for CCI shallow lakes, during 2002-2020. 32
Figure 18. Map of distribution for turbidity trends (orange=positive trend; blue=negative trend; overlaying star=significant trend) for CCI shallow lakes, during the period 2002-2020. 32
Figure 19. Map of distribution for LSWT trends (orange=positive trend; blue=negative trend; overlaying star=significant trend) for shallow lakes, during 2002-2020. 33
Figure 20. Performance of BPNN in all Lakes_cci in terms of RMSE in (a, c) training and (b, d) test sets for all Köppen regions. 35
Figure 21. Feature ranking of meteorological variables in the Köppen regions. 35
Figure 22. Map of Europe showing 36 lakes (green dots) together with (left) surface pressure (Pa) and (right) air temperature (K) on 24 July 2019. Data sourced from ERA5. Modified from Free et al. (2022). 37
Figure 23. Response of three shallow lakes to the double heatwave event. From left to right: Trasimeno (Italy), Võrtsjärv (Estonia), Bolmen (Sweden). (Top) daily air temperature in 2019 (dots with blue smoothed lowess line) and average air temperature (◦C) during 1981–2010 (red dashed smoothed lowess line). (Bottom) Mean lake Chl-a concentration in 2019 (dots with green smoothed lowess line). Yellow box highlights day of year (DOY) between 165–225 (14 June – 13 August). Source: Free et al. (2022). 38
Figure 24. Response of three deep Alpine lakes to the double heatwave event. From left to right: Maggiore (Italy), Constance (Germany/Switzerland), Geneva (France/Switzerland). (Top) Daily air temperature in 2019 (dots with blue smoothed lowess line) and average air temperature (◦C) in 1981–2010 (red dashed smoothed lowess line). (Bottom) Mean lake Chl-a concentration in 2019 (dots with green smoothed lowess line). Yellow box highlights day of year (DOY) during 165–225 (14 June–13 August). Source: Free et al. (2022). 39
Figure 25. Timing (days) and concentration (mg m^{-3}) of peak in Chl-a with respect to the second 2019 heatwave for the three depth lake groups (<7m; 7-15m;>15m). 40
Figure 26. (a) Water level, (b) Chlorophyll-a, and (c) turbidity during 2000 - 2019 in Lake Qadisiyah. 41
Figure 27. Yearly average Chl-a concentration in Lake Qadisiyah. 42
Figure 28. Yearly average turbidity in Lake Qadisiyah. 43
Figure 29. (a) El Niño/Southern Oscillation (ENSO) index (MEI), (b) standardised precipitation index (SPI) in Lake Qadisiyah catchment, and (c) water level during 2000–2019. Red and blue areas in (a) indicate MEI higher than 0.5 and lower than -0.5 respectively. Red and blue areas in (b) indicate SPI higher than 1 and lower than -1 respectively. 44
Figure 30. Time series of the lake surface water temperature (LSWT) anomaly aggregated by continent. 45
Figure 31. Time series of heatwave-days for the global lakes LSWT data set aggregated by continent. 46
Figure 32. Time series of the global lakes ice coverage area aggregated by continent. 46
Figure 33. Overview of browser-based climate indicator dashboard with interactive selection of the indicator, the aggregation method and a country. 47
Figure 34. Time series of ice cover area in Greenland aggregated by lake elevation. 48
Figure 35. Time series of heat wave counts in Sweden aggregated by the water surface area. 49

1 Executive summary

Lakes provide essential aquatic ecosystem services, storing about 87% of liquid surface freshwater on Earth (Messager et al., 2016). However, lake ecosystems are under severe threat worldwide from anthropogenic pressures including climate change. Lakes play an essential role in local and global climate regulation, and they integrate responses to changes in their catchments over time. Since in situ observations of lake proprieties are relatively scarce and unevenly distributed both locally and globally, the use of satellite-derived products can expand and complement measurements across spatial and temporal scales.

In this context, 2024 inland water bodies have been selected for long-term observation records of the Lakes Essential Climate Variables (ECVs), within the European Space Agency (ESA) Climate Change Initiative (CCI), a global monitoring programme aiming to fulfil long-term satellite-based product requirements for climate modelling and observation, set by the Global Climate Observation System (GCOS).

The overarching objective of the Lakes_cci project is to produce and validate a consistent dataset of the thematic variables grouped under the Lakes ECV: lake water level and extent, lake surface water temperature (LSWT), water colour with associated Chlorophyll-a (Chl-a) and turbidity, ice cover and thickness. This includes aiming for the longest period of satellite observations suitable for each specific variable, by designing and operating processing chains that ultimately feature in a sustainable data production system.

A key ambition associated with this objective is to establish wide uptake by a varied and fragmented landscape of potential users. This requires significant alignment of current practices for producing the individual Lakes ECV products, cross-variable validation, data harmonisation and, finally, demonstration in the form of use cases. Successfully tackling the challenge of producing a single data set for the Lakes ECV creates an opportunity to move the science community towards wider uptake of Earth Observation data in limnological studies.

The Lakes_cci project entered its second project phase under the ESA CCI+ programme in 2022. The first phase was largely focussed on harmonisation of effort, upscaling to a set of 2024 inland water bodies, uncertainty characterisation and algorithm improvements. In the second phase, new work started on methodology for the lake ice thickness variable, inter-product consistency checks were implemented, and work on algorithm improvements continues alongside further upscaling of the hydrological variables (water level and extent). To date, the project has issued two major data releases (Climate Research Data Package or CRDP) and associated product documentation. The current project phase will complete in 2025 with a third major data release.

Three prior versions of this Climate Assessment Report (CAR) have been released, whereas this report marks the first issue in the second phase of the project and is associated with version 2.0.2 of the CRDP. This report reviews the Lakes_cci activities and products as performed by the Climate Research Group (CRG) of the project consortium. The CRDP supports different scales of application (e.g., single lake and year, timeseries, regional lake coverage) to meet diverse user needs. This document presents applications of Lakes_cci products and meteo-climatic data, with examples of model integration, across studies from local to regional and global scale, and three specific use cases. Preliminary results illustrate several effects of climate change on lakes, in terms of changes in lake bio-geophysical variables, through temperature anomalies, heatwaves and other extreme events occurring globally. The main findings are summarized as follows:

- at the local scale of Lake Garda, LSWT were both used in LakeVap tool to successfully estimate daily lake evaporation and to prove that the lake is an integrator of noisy climate variability just like oceans are.
- An analysis between lake level and lake quality (i.e. Chl-a and turbidity) in Lake Qadisiyah (Iraq) over the last 20 years showed a potential link between the decrease in water level and El Niño events, which led to reduced precipitations in the lake basin and to drought, with successive decreasing lake water level favouring sediment resuspension and eventually increases in Chl-a and turbidity.
- At regional scale, for 10 south American lakes trend were assessed, suggesting a general increasing trend of air temperature in the region, reflected in a significant increase of LSWT only in three lakes; Chl-a increased in the majority of the lakes, while trends for turbidity were more diverse. Heatwaves and temperature anomalies showed a higher frequency of both positive anomalies and heatwave duration at most southern latitudes.
- The use case on the 2019 heatwave impact on 36 European lakes concluded that timing and magnitude of lake responses depended on lake depth and nutrients, with deeper lakes responding in synchrony with rising temperatures while shallow lakes showing asynchronous responses, with larger algal blooms outside the heatwave period.
- At global scale, shallow lakes trends in bio-physical variables suggested that these lakes are getting more turbid and with increasing of Chl-a. A machine learning approach was tested on the 2024 lakes, revealing that day of the year (DOY) and solar radiation are the main predictors of LSWT variability.
- The dashboard developed for climate indicators allowed to investigate several use cases such as the detection of a significant decrease of ice cover in lakes in Greenland and the observation of heatwaves increase in frequency and intensity in Swedish lakes over recent years.

2 Introduction

2.1 Purpose of this document

This document summarizes the current activities within the Lakes_cci project both in the context of CRDP assessment and evaluates how the project meets the user requirements as defined by the climate modelling user group (CMUG) and the wider community of lakes scientists and stakeholders (URD v1.0). The overall purpose of the document is to summarize the value of Lakes_cci products and related activities for climate science.

This is the first version of the CAR to evaluate CRDP v2.0. The next update will be in 2025, assessing CRDP v3.0.

2.2 Structure of the document

The first part of the document introduces the products generated in the Lakes_cci. The second part provides a first assessment of these products. Three sections are then dedicated to the use of the products at local, regional, and global scales.

- Local scale assessment: Lake Garda (Italy).
- Regional scale assessment: South American lakes.
- Global scale assessment: Trends of water quality in shallow lakes; Meteorological factors influencing LSWT across different climates.

A section on the Use Cases outcomes is presented as follow:

- Heatwave and storm event impacts on lakes.
- La Niña influence on water quantity and quality of a reservoir in a hot desert climate (Lake Qadisiyah, Iraq).
- Aggregated climate indicators for the global lakes dataset: Ice cover Greenland; Heatwaves Sweden.

A section followed with an update on user requirements and user workshop activities, a dedicated section evaluates externally published work. Finally, a section presents key conclusions.

3 Products of the Lakes_cci

Lakes_cci is developing the latest generation satellite Earth observation products for a set of 2024 inland waterbodies distributed globally. The data set contained in CRDP v2.0.2 spans 1992 to 2020 for some variables, or shorter periods as satellite assets allow. The data set is supplied in the same temporal and spatial framework in NetCDF format and makes up the Lakes Essential Climate Variable (ECV) with the following products:

- Lake Water Level (LWL)

Lake Water Level is the measure of the absolute height of the reflecting water surface beneath the satellite with respect to a vertical datum (geoid) and expressed in metres. LWL is a fundamental proxy to understand the balance between water inputs and water loss and their connection with regional and global climate changes.

- Lake Water Extent (LWE)

Lake Water Extent refers to the extent (or area) of a lake covered by water, it is a proxy for change in glacial regions (lake expansion) and drought in many arid environments. Water extent can influence the local climate, for example having a cooling effect. This variable can also provide information for ongoing processes in the littoral zone of a lake, crucial for lake catchment-basin interactions and key habitat for many biological communities.

- Lake Surface Water Temperature (LSWT)

The Lake Surface Water Temperature LSWT is defined as the temperature of the water at the surface of the water body (surface skin temperature). LSWT is correlated with regional air temperatures and can be a proxy for mixing regimes, driving biogeochemical cycling and seasonality.

- Lake Ice Cover (LIC)

Lake ice cover (LIC) refers to the extent (or area) of a lake covered by ice. Timing of freeze-up in autumn and advancing break-up in spring are proxies for gradually changing climate patterns and seasonality.

- Lake Ice Thickness (LIT)

Lake Ice Thickness (LIT) can be considered a driver of seasonal lake biogeochemistry and early indicator of changing lake thermodynamics.

- Lake Water Leaving Reflectance (LWLR - Chlorophyll-a and turbidity)

Lake Water-Leaving Reflectance (LWLR), also referred to as water colour, is the measurement of the quantity of sunlight reaching the remote detector after interaction with the water column. From LWLR, chlorophyll-a (Chl-a) and turbidity have been derived. LWLR represents a direct indicator of biogeochemical processes in the visible part of the water column (e.g., seasonal phytoplankton biomass fluctuations and blooms) and can be used to trace the frequency of extreme events (e.g., peak terrestrial run-off, changing mixing conditions).

Each of the Lakes ECV products has associated uncertainty estimates.

Given the diversity of variables and methods used to collect, analyse and provide the data, we recommend reading the following documents prior to using the Lakes_cci dataset.

- Product User Guide (PUG).
- End-to-End ECV Uncertainty Budget (E3UB).
- Algorithm Theoretical Basis Document (ATBD).
- Product Specification Document (PSD).

4 Data exploration

The data presented in this CAR are based on the second version (v2.0.2) of the dataset for 2024 inland waterbodies. 84% of the dataset target lakes and 16% are reservoirs – the term lakes is used to describe both for the purpose of this assessment. A descriptive table of all locations and the availability per ECV product is provided through the project website[1]. The data set has improved product quality filters and flags and coverage of Lake Water Level and Lake Water Extent compared to the previous release (v1.0.0). The merged satellite products (Carrea et al., 2023a) have the following main characteristics:

- Daily aggregation interval pinned to 12:00:00 UTC.
- Grid format with spatial resolution of 1/120 degrees (near 1 km at the equator).
- Per-lake variables (LWL and LWE) are duplicated into the grid for the area given under the nominal spatial delineation of that lake, derived from its maximum water extent as used for the variables resolved for the whole lakes grid.
- Datum: WGS84.
- Extent: -180 to 180 degrees longitude, -90 to 90 degrees latitude, where positive signs point north and east. The pixel coordinate is the centre of the pixel. This results in 21600 grid rows and 43200 grid columns.
- Spatial coverage: 2024 globally distributed lakes.
- 1 netCDF file per day containing all thematic variables.
- Temporal coverage: from 1992 up to 2020 (LWL/LWE: 1992-2020; LIC/LIT: 2000-2020; LSWT: 1995-2020; LWLR: 2002-2020).

CRDP V2.1.0 is scheduled for dissemination in February 2024. The temporal coverage of that data set will be extended to the year 2022. Some further expected changes are:

- LWL/LWE: increased spatial coverage and better temporal coverage for some lakes using additional data from past missions.
- LSWT: reprocessed SLSTR/Sentinel3A/B for CRDP v2.1 and found slight degraded performance for SLSTRA in 2021 and 2022; therefore, SLTRA was excluded, and dataset created with SLTRB and MODIS.
- LIC: increased temporal coverage.
- LIT: new product added for demonstration over Great Slave Lake only.
- LWLR: new quality flags for LWLR including from inter-product consistency checks, and harmonisation of variable naming for wavebands in close proximity but on different sensors.

4.1 The Lakes_cci data at a glance

4.1.1 Spatial distribution

The global distribution of the lakes included in V2.0.2 is shown in Figure 1. Of the 2024 waterbodies 1697 are classified as lake, 325 as reservoir, 1 salt marsh and 1 wetland area (drying lake).

[1] https://climate.esa.int/en/projects/lakes/data

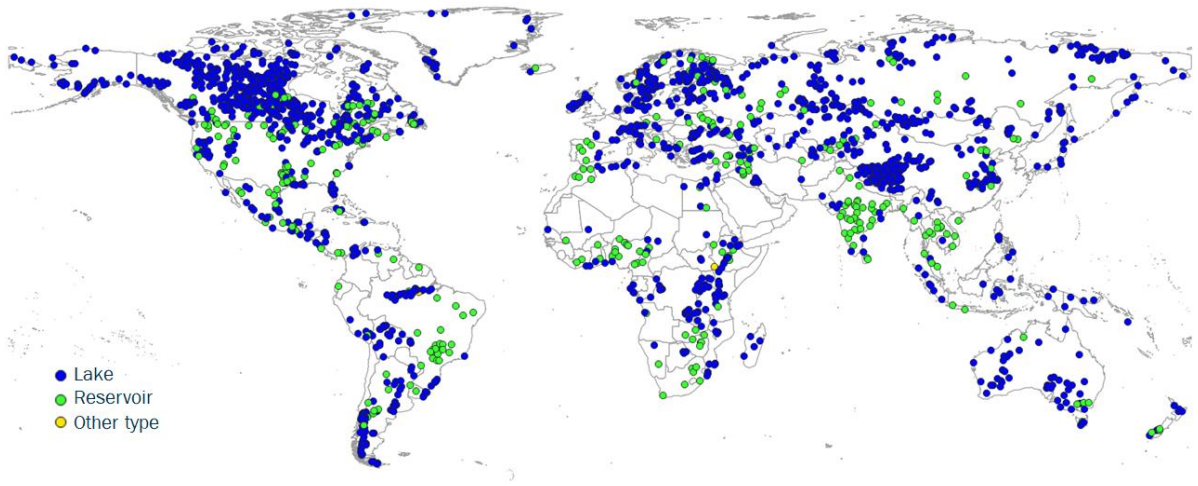

Figure 1. Global distribution of the Lakes_cci dataset (v2.0.2). Other type: i) Rio Tapajaos and Rio Arapiuns complex, Brazil; ii) West Ngalabalab swamp, Sudan.

4.1.2 Global distribution of ECVs

Satellite products for the 2024 lakes extracted from the NetCDF files were used to illustrate the temporal distribution of each thematic variable across the years. Uncertainty layers associated with the ECVs were used to filter the data. The level of acceptable uncertainty is application-specific and for this exploration we used the criteria listed in Table 1, following the approach applied in the previous CAR (2021).

The following data processing steps were performed:

- Filtering data (water temperature, water level, water extent, Chl-a, turbidity) according to associated uncertainty/quality indicators (Table 1). A level of 60% uncertainty was used to filter data for Chl-a as this corresponded to retaining the 90% of the data and rejecting the 10% where uncertainty exceeded 60%. A level of 70% uncertainty was used to filter data for turbidity as this corresponded to retaining the 90% of the data and rejecting the 10% where uncertainty exceeded 80%.
- Extraction of mean values based on lake vector definitions.
- Removal of Chl-a and turbidity data when ice cover data is also present to avoid ice interference on water quality data.
- Threshold settings: i) LSWT, values < 200 K and > 374 K; ii) Chl-a, values <0.0001 mg m^{-3} and >300 mg m^{-3}; iii) turbidity, values <0.0001 mg m^{-3} and >1000 mg m^{-3}.
- Removing extreme outliers (>5 times the inter-quartile range, IQR).
- Conversion to time series.
- Calculating monthly and annual averages.
- Some variables were normalised for allowing comparison (described below).

Table 1. Quality control filters used when extracting data for this assessment.

Thematic variable	Applied approach
Temperature	Selection limited to LSWT quality level 4 – 5.
Level	Filtered by 0.1m of uncertainty.
Extent	Error is standard value per lake – not filtered.
Chlorophyll-a	Filtered by an uncertainty of 60%.
Turbidity	Filtered by an uncertainty of 70%.

Plots indicating the data distribution over time, calculated per lake, are shown in Figure 2, Figure 4, Figure 5, and Figure 6.
For Chl-a, turbidity and LSWT the annual average calculated per lake was also compared to the previous product version. Data seasonality is not considered in this analysis. The distribution plots are here proposed to examine consistency in data distribution for the different Lakes_cci products, and not intended to explain global climatic trends.
Data distribution of LWL for the global dataset is reported separately for lakes and reservoirs, with normalised data calculated as annual average divided by time-series average.
For LWE data, a suitable global data distribution plot cannot be produced because of the low number of available observations in the dataset.
The distribution of Chl-a concentration, presented as the annual average per lake, is shown in Figure 2 for both CRDP v1.1 (250 lakes) and CRDP v2.0.2 (2024 lakes). Some outlier Chl-a values have been removed for visualisation purposes. The gap between 2012 and 2016 is due to the end of life of ENVISAT-MERIS sensor and the launch of the new Senintel3-OLCI sensor. This gap was preliminary filled for about 40 lakes with MODIS data. For this reason the global graph distribution is reported with this 4-year gap. While the v1.1 dataset was unimodal with most of the concentrations centred around 10 mg m^{-3}, the v2.0.2 dataset shows a broader distribution, particularly for the period 2002-2012, with concentrations centred around 10 mg m^{-3} and a smaller peak around 4 mg m^{-3}. This change in values distribution was likely due to the addition of a significant number of lakes in oligotrophic conditions. No specific direction of change in Chl-a was observed for the global dataset over time.
Some spatial patterns in the variation of lake trophic status were visible (Figure 3). In particular, lakes in oligo- and ultra-oligotrophic conditions were concentrated in the southern part of South America and in the Tibetan plateau, and in alpine areas, potentially representing a global refuge for lakes close to pristine status. In contrast, there was a higher frequency of lakes of hypertrophic status in central Europe, Russia and North America, where eutrophication pressures on lakes are known to be higher. Lake concentrations and trends of Chl-a may vary depending on specific anthropogenic pressures in lake catchments like land use and nutrients load, with potential synergic effects by climate change.

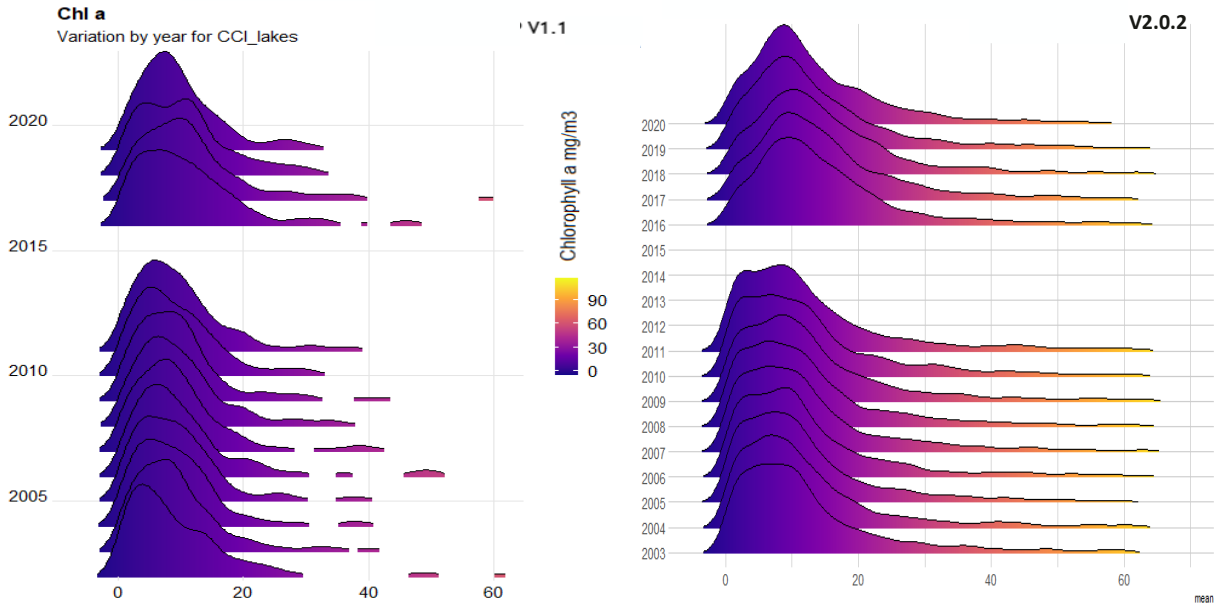

Figure 2. Distribution of Chl-a concentration, annual average calculated per lake, for CRDP v1.1 (250 lakes) from 2002 to 2019 (left) and for v2.0.2 (2024 lakes) from 2002 to 2020 (right). Some outlier values of Chl-a have been removed for clarity.

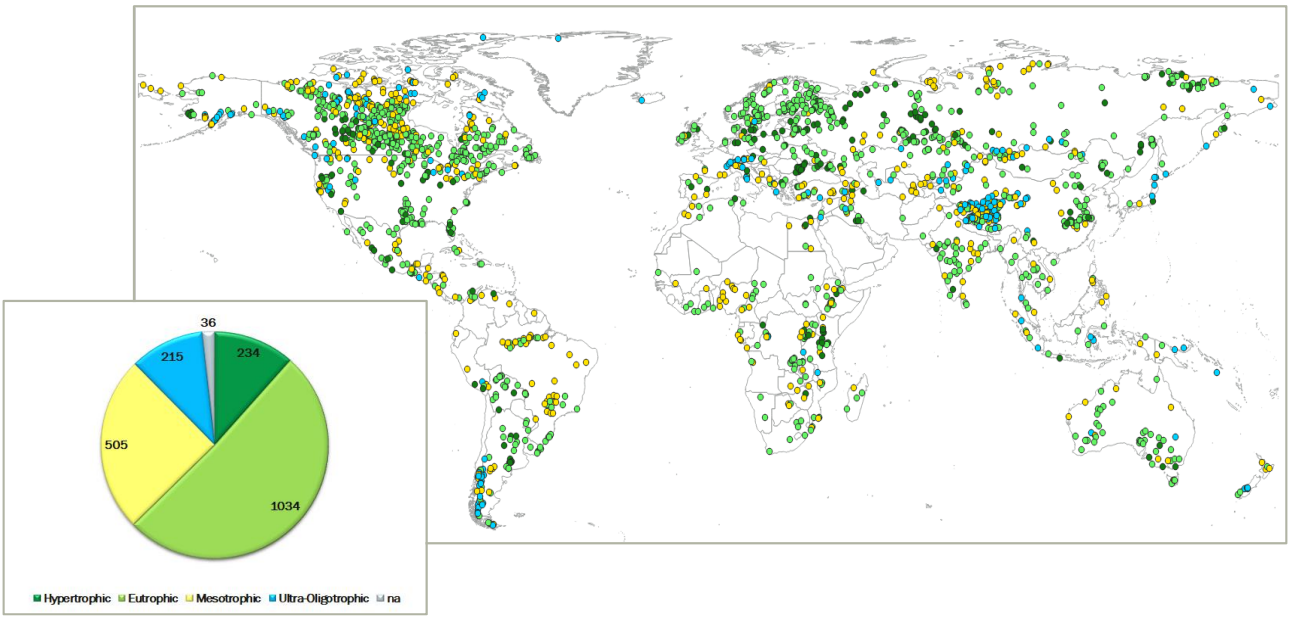

Figure 3. Lake trophic status classification based on the average Chl-a concentration (mg m^{-3}) for the global dataset (V2) from 2016 to 2020. In the pie chart the number of lakes per category is reported.

Distributions of turbidity (NTU) as derived from the annual average per lake, for both CRDP v1.1 and v2.0.2, are reported in Figure 4. Some outliers have been removed for clarity. In both datasets turbidity distribution was unimodal with concentration centred around 2 NTU.

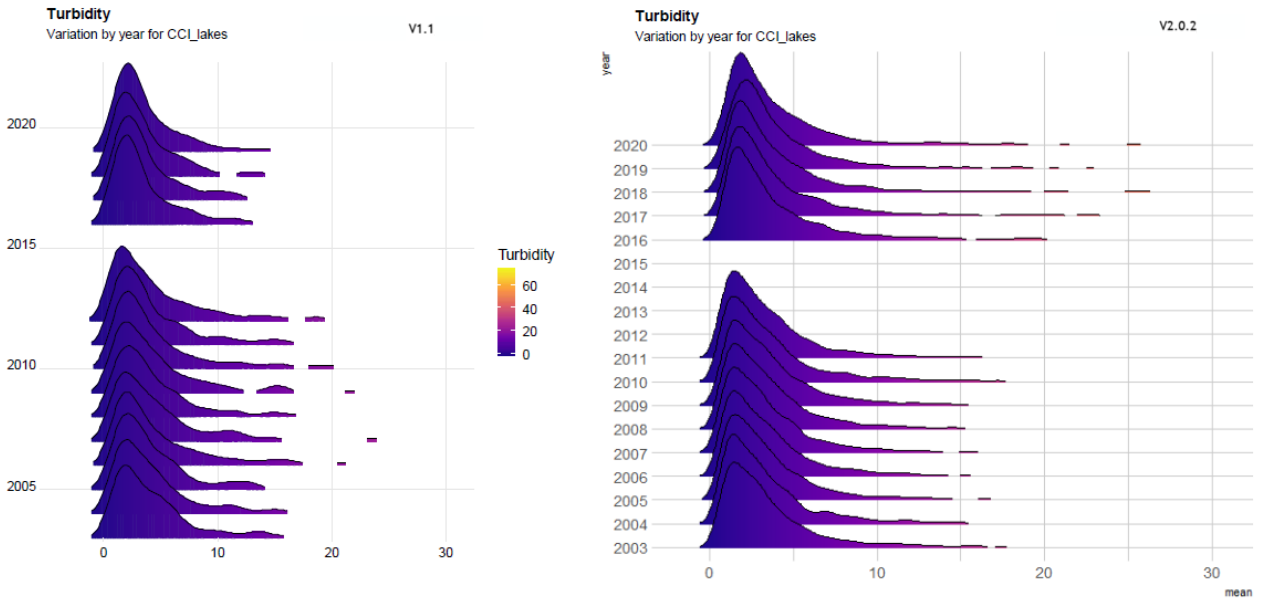

Figure 4. Distribution of turbidity (NTU), annual average calculated per lake, for the global dataset V1.1 (250 lakes) from 2002 to 2019 (left) and for dataset 2.0.2 (2024 lakes) from 2002 to 2020 (right). Some outliers were removed for clarity.

Global distributions of lake surface water temperature (LSWT; °C) are shown in Figure 5, as the annual average calculated per lake, for the previous and current data set. Note that bimodal distributions are derived from lakes being either close to temperate or equatorial regions. While the peak in v1.1 was

centred at ≤ 10 °C, v2.0.2 shows a shift to around 14 °C, likely because of the larger addition of lakes in temperate regions.

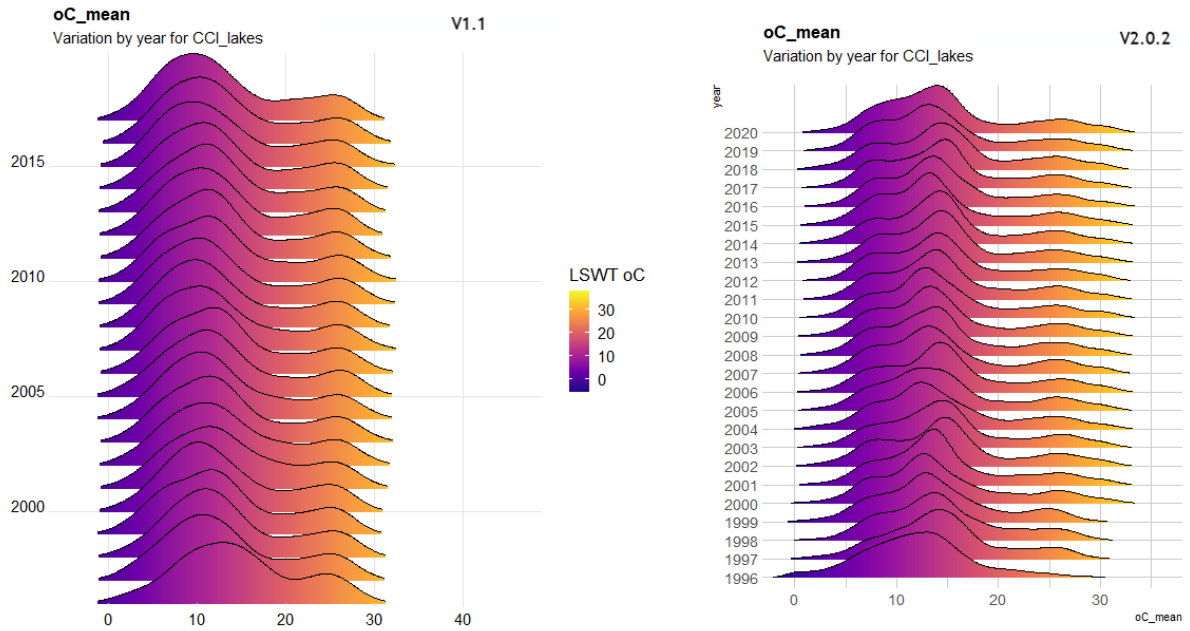

Figure 5. Distribution of lake surface water temperature (LSWT; °C). Annual averages calculated per lake, for (left) CRDP v1.1 (250 lakes) from 2002 to 2019 and (right) CRDP v2.0.2 (2024 lakes) from 2002 to 2020. Note that bimodal distributions are derived from lakes being either closer to temperate or equatorial regions.

The distribution of normalised LWL is determined from the per-lake annual average divided by their time-series average for CRDP v2.0.2 is shown in Figure 6. Lakes (natural and controlled) and reservoirs are shown separately. For lakes, the LWL distribution is centred around 100%, and it is stable over time; while for reservoirs the LWL distribution has a wider range between 98% - 102% in the investigated period.

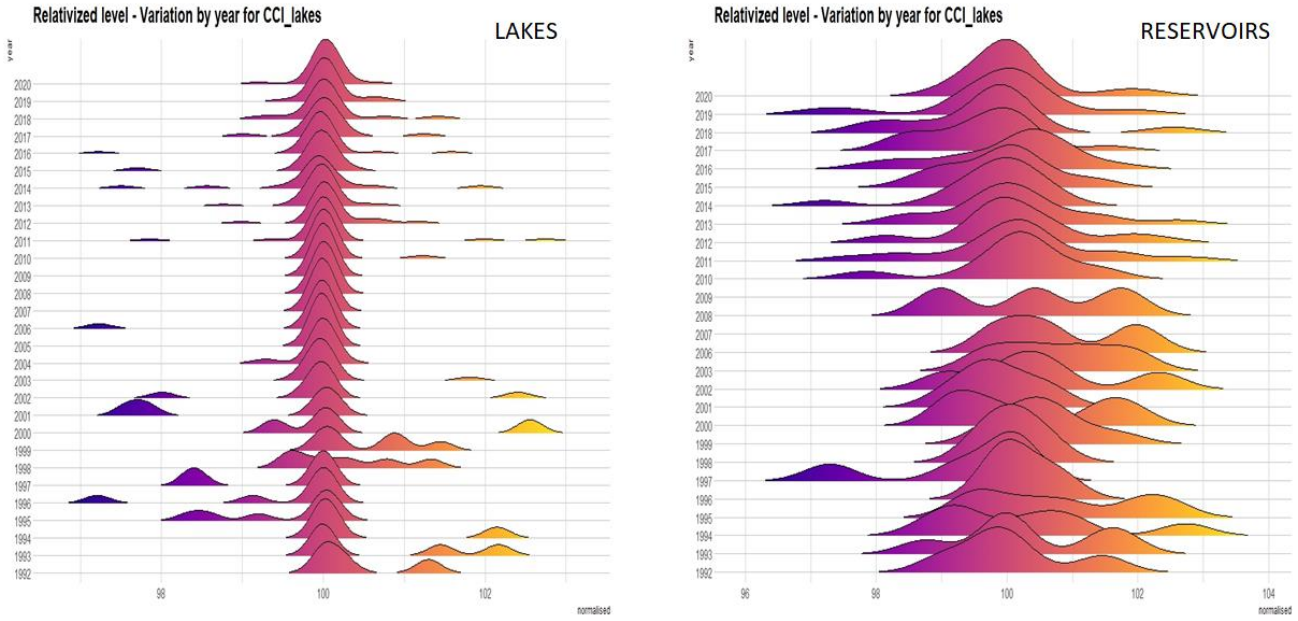

Figure 6. Distribution of normalised (%) lake level, calculated per lake (left) and reservoir (right) typology as annual average divided by time-series average, for the global dataset. Scaled between 96-104% for clarity.

5 Local-scale assessment

5.1 Lake Garda (Italy)

A series of specific applications of use the Lakes_cci dataset are demonstrated for Lake Garda, a deep clear lake in the subalpine ecoregion and the largest lake of Italy. Lake Garda is situated in the Po River catchment and is an essential water source for agriculture and other use. It functions as a reservoir for crop irrigation, livestock, hydroelectric power production, drinking water, among other uses such as tourism. Lake Garda has been studied extensively using satellites, field measurements and hydrodynamic modelling, hence providing a suitable test case for exploring Lakes_cci data in detail. We note that validation of the dataset is not the aim of this document, interested readers should instead refer to the Product Validation and Algorithm Selection Report (PVAR) and Product Validation and Intercomparison Report (PVIR).

Two studies are presented in the following sections.

5.1.1 Satellite-based evaporation mapping

At all latitudes and climates, evaporation from water surfaces is a key component of the overall budget of heat and water volume in natural and artificial reservoirs. Under the perspective of global warming, drying climate and water scarcity, several studies have projected a general increase in lake evaporation (Wang et al. 2018, Woolway et al., 2019) due to the alteration of environmental drivers sensitive to climate change such as e.g. air and water temperature, air vapor content, wind speed and solar radiation (Vystavna et al. 2021). How and to what extent evaporation from lakes increases, varies worldwide (Zhou et al. 2021, Zhao et al. 2022), as the hydroclimatic variables involved in this process depend on the climatic region (Peel et al. 2007) and on lake thermal behaviour (Maberly et al. 2020). Many investigations in the scientific literature address this issue in arid and semi-arid contexts, where lakes suffer from water deficit when evaporation exceeds precipitation, thus implying in some cases significant groundwater uptake to compensate the water balance (e.g. Riveros-Iregui et al. 2017). However, lake evaporation is an issue at medium and high latitudes as well. At high altitudes (e.g. in the Tibetan Plateau), lake evaporation tightly interacts with increasing trends of precipitation and glacier melting and contributes to the expansion of new lakes (Yang et al. 2018; Guo et al. 2019). In temperate to boreal environments, evaporation is strongly correlated with the duration of the ice-cover period, whose climate-induced reduction is leading to a general increase of evaporation losses for many lakes of this kind (e.g. Lake Superior: Blanken et al. 2011, White Bear Lake: Xiao et al. 2018).

As evaporation from lake surfaces interact with all such physical properties of lakes, the use of globally consistent variables such as those included in the Lakes_cci dataset (LSWT, LIC, LWL) can be of extraordinary support for the estimation of evaporation trends worldwide. In a paper by Matta et al. (2022), we used the LSWT dataset to develop and test a simple satellite-based tool named LakeVap specifically designed for mapping evaporation from lakes and reservoirs. The model was tested on Lake Garda (Italy) by combining the long time series of LSWT to different sources of meteorological forcing. We discussed the role of spatial variability, data availability and quality and operative application in the production of lake evaporation maps.

LakeVap (Figure 7) estimates the heat flux associated to evaporation at satellite overpass time based on the bulk transfer theory (Dalton 1802). We used the formulation by Fink et al. (2014) and considered surface water temperature, wind speed, air temperature, relative humidity. From the instantaneous latent

heat flux (W/m²), the hourly rate of evaporation is then obtained in *mm/h* in each pixel of the maps. Through the integration of a simplified energy balance over 1hr time intervals, LakeVap can also compute daily evaporation rates in mm/d by simulating the rate of warming/cooling of LSWT in the 23 hours after the satellite overpass time.

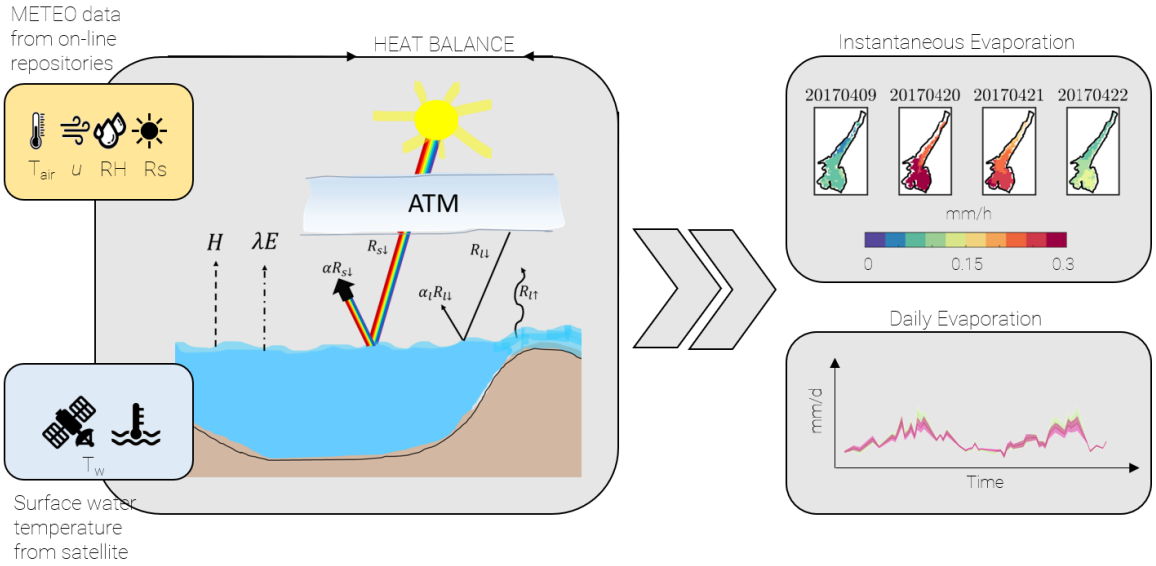

Figure 7. Workflow for the generation of evaporation products from LSWT maps. Left: Schematic of the terms of the heat balance in a water body and data sources. Right: example of maps of instantaneous evaporation in mm/h and time series of spatially averaged daily evaporation in mm/d. Figure modified from Matta et al. (2022).

An example of the instantaneous evaporation maps that can be obtained with the LakeVap tool from Lakes_cci LSWT maps and ERA-5 meteo data in year 2017, for which 99 images are available, is shown in Figure 8. The time series allows observing the seasonal evolution of evaporation. Evaporation in Lake Garda typically increases from the beginning of the year until June to September, when the difference between air and water temperature is maximum, and then decreases again in late autumn and winter. This behaviour is consistent with that observed in similar lakes (e.g. Lake Constance: Fink et al. 2014, Lake Geneva: Rahaghi et al. 2018, Vercauteren et al. 2009). This behaviour is found every year and is related to the seasonal evolution of LSWT and to the thermal capacity of the lake, which stores heat during days of intense solar radiation and then slowly gives it off in the following days and months. However, unexpected maxima in winter (January) or early spring (April) or late autumn (November) can be found when strong synoptic winds sweep over the lake enhancing evaporation, often associated with exceptionally cool and dry days, when air temperature and relative humidity are way lower than the mean climatological conditions (Blanken et al. 2011).

In terms of spatial variability, Matta et al. 2022 show that LSWT spatial gradients of -4/+8% (10th/90th percentiles) are found on average throughout the year. If all meteorological variables are taken as spatially averaged, such gradients determine an average variability of +-20% in evaporation at basin scale. However, for the specific case study, also meteorological forcing greatly vary spatially, as longitudinal gradients are typical in Lake Garda. Air and water temperatures indeed tend to be warmer in the southern part and colder in the northern part, where stronger winds typically develop due to thermal breezes from north to south at the acquisition time of Lakes_cci dataset sensors. Thus, the final spatial distribution of evaporation is dependent on all contributions. We conclude that the information from a spatialized dataset of LSWT such as the CCI one is relevant for our case study for correctly describing the

spatial variability of evaporation and is expected to be even more critical in those contexts where more homogeneous atmospheric forcing overlies heterogeneous LSWT fields.

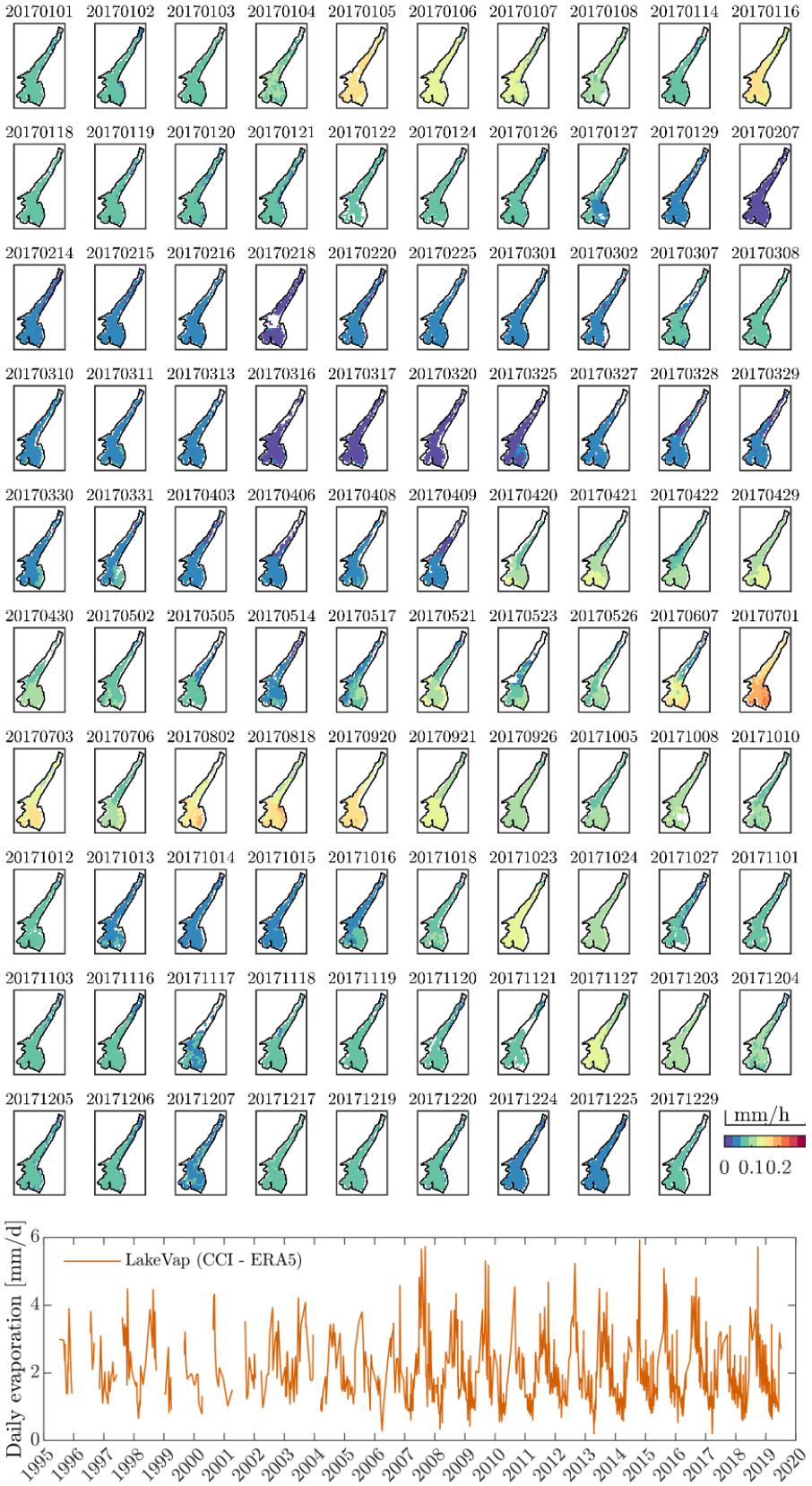

Figure 8. Top: hourly evaporation from Lake Garda estimated with the LakeVap tool in year 2017 fed by Lakes_cci LSWT maps and ERA5 meteorological data. Bottom: daily evaporation from Lake Garda (spatial average from daily evaporation maps). The gaps in the time series highlight when LSWT maps are not available for more than 60 consecutive days. Figure modified from Matta et al. (2022).

With the increase of evaporation projected for water bodies worldwide, there is a growing need for flexible and low data-demanding tools enabling the monitoring and management of water resources. In the range of available methods for estimating evaporation, the least demanding ones only need air temperature and solar radiation, while the most accurate, demanding and expensive ones require a full array of in-situ measurements (e.g. via Eddy Covariance towers). LakeVap only needs LSWT (at satellite overpass time) and a few atmospheric variables, which can be obtained from reanalysis such as ERA5. This makes LakeVap a "low data-demanding" tool. In Matta et al. 2022, we demonstrate that the daily estimate of LakeVap is comparable to that of a full 3D hydro-thermodynamic model providing hourly resolution results and requiring bathymetry, in-situ temperature profiles and all atmospheric variables. Building on this, the LakeVap tool can be applied for any case study included in datasets such as Lakes_cci without the need of additional information, as it is combined with global atmospheric/land models such as ERA5-Land with a worldwide coverage.

5.1.2 Spatio-temporal bio-geophysical surface features

Lake Surface Water Temperature (LSWT) is associated with the skin layer (< 1 mm) such that a direct comparison with in situ data will incur a bias (Wilson et al. 2013). Recent applications have shown the potential of the spatio-temporal variability of LSWT for investigating subsurface dynamics, e.g. mixing regime shifts (Fichot et al. 2019). Consolidated studies in the ocean (Frankignoul and Hasselmann 1977) largely demonstrated that Sea Surface Temperature (SST) carries information on the surface mixed layer, which reacts to atmospheric white noise by damping high frequency forcing and leading to a red noise SST response. The color "red" is associated to the spectrum of SST anomalies in analogy with the visible spectrum and refers to the fact that the signal shows higher power in longer wavelengths, with a $\frac{1}{f^2}$ frequency spectrum.

In a paper by Amadori et al. (2023), we investigate the possibility to gather information on subsurface thermal complexity by analysing the spatiotemporal variability of remotely sensed products. Lake Garda is characterised by deep clear waters, and a long time series of biophysical observations from both satellite and in situ efforts is available, as well as consolidated knowledge of its main morphological features and thermal behaviour. We assess the dominant spatiotemporal modes of variability for LSWT, chlorophyll-a (Chl-a) and turbidity products from the Lakes_cci, and compare the obtained patterns with that of the thickness of the well-mixed surface layer as estimated from the LSWT anomaly using Hasselman's theory (Hasselman 1976, Frankignoul and Hasselmann 1977).

Data selection / discard criteria followed recommendations in the PUG. Gap-filling was performed in space with a nearest neighbour interpolation and in time with a linear interpolation between resampled time series at 2 days temporal resolution for LSWT and 10 days for Chl-a and turbidity. We then pre-processed the data such that each pixel has zero mean and no seasonal variability. Empirical Orthogonal Functions (EOF) analysis was performed on the detrended and de-seasonalised spatial anomalies of LSWT, Chl-a and turbidity in order to get the dominant modes explaining the spatiotemporal variability of these quantities.

For LSWT and Chl-a, the first dominant mode (EOF1) has a dipole pattern between the northern and southern basins of Lake Garda (Figure 9), suggesting that these two areas are anti-correlated one-another. The two maps have a cross-correlation of 0.83. EOF1 of turbidity shows a different pattern, with the two anti-correlated basins longitudinally displaying an east-west gradient. We argue that the pattern observed in Figure 9 (panels a-b) is due to different thermal behaviour of the two sub-basins and can be

interpreted as mixed layer depth variability, which affects the surface temperature as well as Chl-a dynamics, while not having significant effects on turbidity in Lake Garda.

To test this hypothesis, we assumed that LSWT anomalies in Lake Garda can be represented as a first order autoregressive model (AR1) whose autocorrelation function between observations *k* time periods apart has an exponential behaviour of the kind: $e^{-\gamma k \Delta t}$, with k= lags (Figure 10). Hence, we fit the autocorrelation of the time series of detrended and de-seasonalized LSWT in each pixel of the map to estimate γ. From γ we estimate the scale of the mixed layer depth (MLD) following Frankignoul and Hasselmann (1977). Results presented in Figure 5.1.6 show that the exponential theory fits the behaviour of LSWT anomalies well (panel a, $R^2 > 0.9$), and that the estimated mixed layer depth has a clear spatial pattern resembling the bathymetry of the lake and the dominant EOF1 of LSWT and Chl-a (Figure 9a,b).

The estimated MLD is consistent with in situ measurements during the stratified season and supports the hypothesis that LSWT and Chl-a carry the information on the different thermal regimes of the lake, which is oligomictic in the north-western basin (deeper MLD) and monomictic in the south-eastern basin (shallower MLD). Such differences were already observed in situ (Milan et al. 2015), with remote sensing (Bresciani et al. 2011), models (Amadori et al. 2021, Matta et al. 2022), and are common to other multi-basin lakes (e.g. Lake Lugano: Lepori et al. 2018). Our results also show, for the first time in a lake, that LSWT variability can be explained as an integral response to atmospheric white noise. This behaviour allows determining a scale of mixed layer depth and identifying a signature of the main spatial patterns of remotely sensed water quality parameters, revealing underwater heterogeneity and opening to a new perspective for EO-based climate studies.

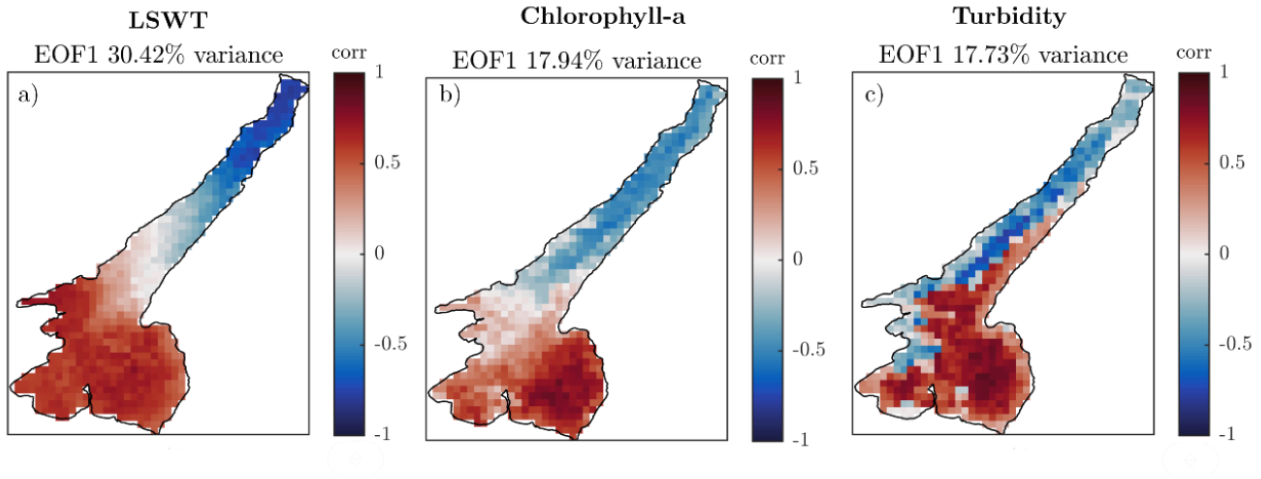

Figure 9. First dominant mode (EOF1) from LSWT (a), Chl-a (b) and turbidity (c) from Empirical Orthogonal Function analysis on anomalies.

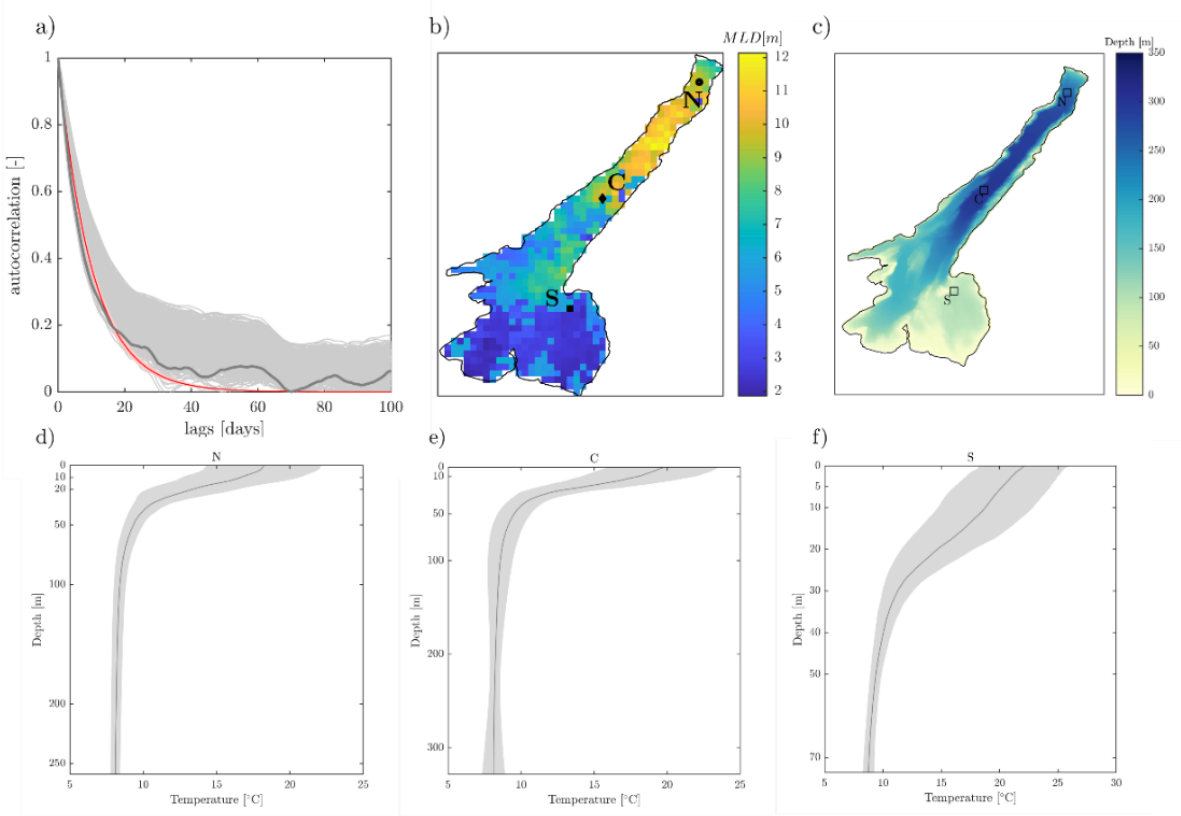

Figure 10. (a) autocorrelation functions of LSWT anomalies in each pixel of the maps (grey lines), of the spatial mean of LSWT anomaly (thick grey line) and corresponding exponential fitting (red line). (b) map of MLD estimated with Hasselman's theory; (c) bathymetry; (d-f) thermal profiles from three in situ observations (black dots in (b) map).

6 Regional-scale assessment

6.1 South American lakes

6.1.1.1 Trend analysis

South America has one of the highest levels of biodiversity on the planet (Castellanos et al. 2022). Land use changes in the region are significant, particularly deforestation, and additional land pressures from pollution and induced fires exacerbate the impacts of climate change both on land and water resources. The region boasts the largest tropical forest on the planet and other important biomes of high biodiversity on mountains, lowlands and coastal areas. Climate projections indicate increases in temperature for the entire region by 2100 for RCP4.5 and RCP8.5, but rainfall changes will vary geographically (Castellanos et al. 2022).

The highest abundance of tropical mountain lakes occurs in the South American Andes, where recent climate change has outpaced most other parts of the planet (Vuille et al. 2003). Air temperatures in the Andes are exceeding the upper limits of variability documented by historical meteorological data (Michelutti 2015), and climate related changes are impacting Andean water resources via alterations to the amount and patterns of regional precipitations (Thibeault et al. 2010; Vuille et al. 2003), and reduced runoff from rapidly melting glaciers (Rabatel et al. 2013; Vuille et al. 2008).

South America shows increasing trends of climatic change and variability and extreme events severely impacting the region, with potential consequences on lakes.

To explore water conditions and changes in lakes during the last two decades in South America we selected a group of ten lakes in different geographical and climatic sub-regions, covering different ecological settings (Table 6.1.1). The lakes were selected out of 172 lakes in the Lakes_cci dataset for the region. The HydroLAKES database was used to characterize the selected lakes, as it provides the main hydro-morphological characteristics for lakes with a surface area of at least 10 ha. The five largest Regions of Interest (5-ROI) per lake were created based on the JRC Global Surface Water Explorer (GSW) occurrence layer[2]. For the period 2017-2020, the weighted mean (by pixel number) per day per lake was calculated for Chl-a concentrations and turbidity. This method ensured that the pixels considered were likely free from ice cover, macrophytes, islands and extremely shallow waters. The proportion between the area of the 5-ROI and the Lakes_cci data coverage was calculated, and three groups were made based on the percentage of cover of these ROIs of the total lake surface: (1) >80% consisting of 10 lakes, (2) >70% consisting of 21 lakes, and (3) >60% containing 40 lakes. We selected firstly 10 between lakes and lagoons of the first cover group (>80%), with a successive substitution of two lagoons with two lakes from greater than 70% cover group and one lake from greater than 60% cover group, in order to keep a representative number of lakes in the subset for our analysis.

South America is a diverse continent in terms of geomorphology and climates, which in turn translates into a wide diversity of lake types. Additionally, hydroelectric power generation is of paramount importance in this continent (Llames and Zagarese 2009). The selected water bodies included six natural lakes, two reservoirs and two lagoons, covering a range of trophic conditions (from ultra-oligotrophic to eutrophic), morphological types (from shallow to deep lakes) and five climatic sub-regions (including tropical, coastal and mountain areas) spanning a wide latitudinal range (from 4.7°S to -49.6°S). Figure 11 shows the map of distribution, names and Lakes_cci id of the 10 selected lakes in South America.

[2] global-surface-water.appspot.com

Table 1 illustrates the main lake morphological characteristics and local importance in ecological services and water uses of the selected lakes.

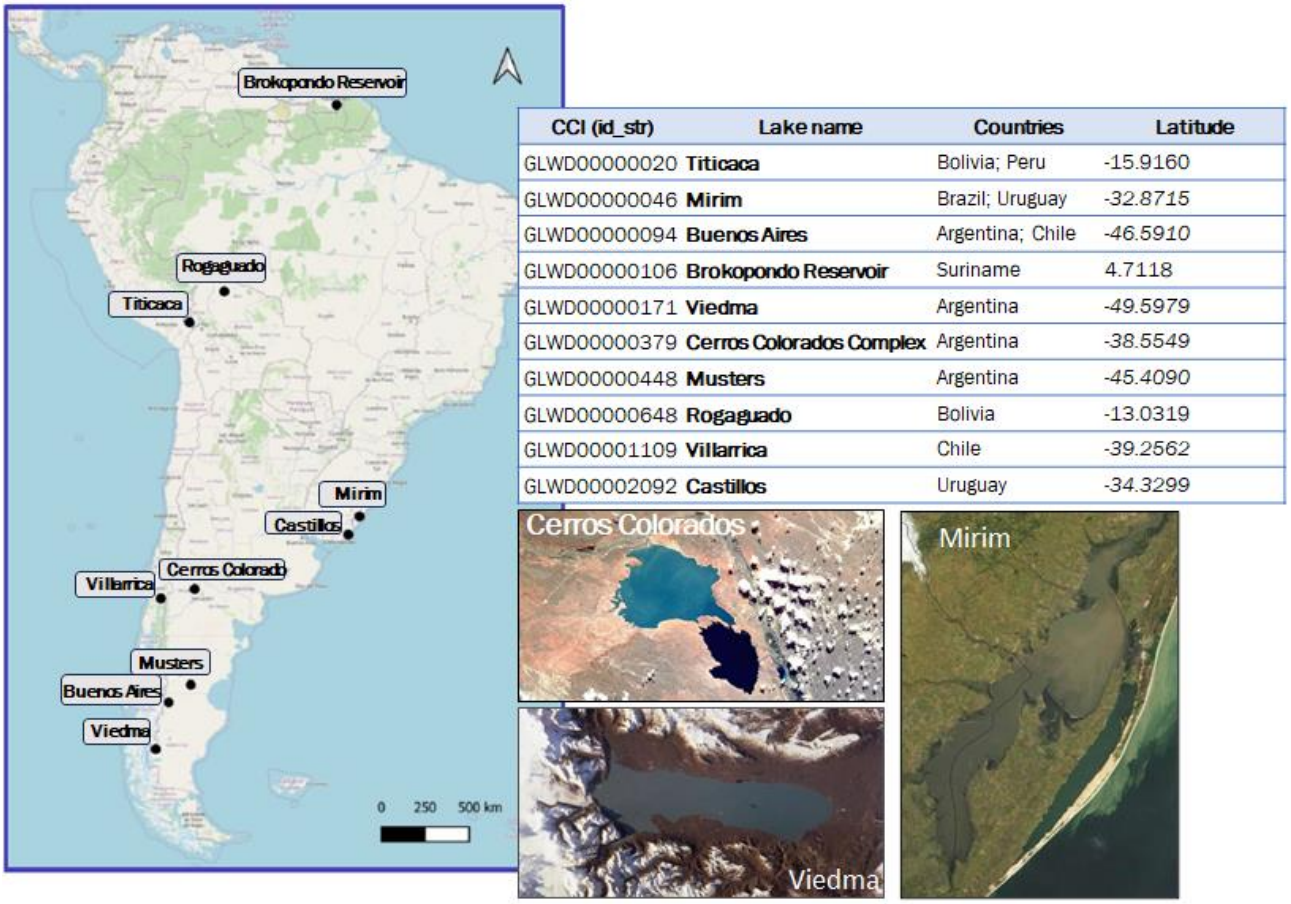

CCI (id_str)	Lake name	Countries	Latitude
GLWD00000020	**Titicaca**	Bolivia; Peru	-15.9160
GLWD00000046	**Mirim**	Brazil; Uruguay	-32.8715
GLWD00000094	**Buenos Aires**	Argentina; Chile	-46.5910
GLWD00000106	**Brokopondo Reservoir**	Suriname	4.7118
GLWD00000171	**Viedma**	Argentina	-49.5979
GLWD00000379	**Cerros Colorados Complex**	Argentina	-38.5549
GLWD00000448	**Musters**	Argentina	-45.4090
GLWD00000648	**Rogaguado**	Bolivia	-13.0319
GLWD00001109	**Villarrica**	Chile	-39.2562
GLWD00002092	**Castillos**	Uruguay	-34.3299

Figure 11. List and map of distribution of the 10 selected lakes in South America. Latitude in italics in the table refer to lakes at latitude <-23.5 used as threshold for LSWT trend analysis.

Table 1. Lake name, type, area, average depth, trophic status, ecosystem services and main uses for the subset of South American lakes investigated. The reference reported are listed as footnotes[3].

---

[3] [1] Lake Titicaca. (n.d.). Global Nature Fund. Retrieved November 29, 2023, from https://www.globalnature.org/en/lake-titicaca

[2] Data List - Lake Titicaca. (n.d.). International Lake Environment Committee - World Lake Database. Retrieved November 29, 2023, from https://wldb.ilec.or.jp/Lake/SAM-04/datalist

[3] Pinto, F. P., Tormam, M. F., Bork, C. K., Guedes, H. A. S., & Silva, L. B. P. D. (2020). Seasonal assessment of water quality parameters in Mirim Lagoon, Rio Grande do Sul State, Brazil. Anais Da Academia Brasileira De Ciencias, 92(3), e|20181107. https://doi.org/10.1590/0001-3765202020181107

[4] Borges, E. L., Kunst-Valentini, M., dos Santos, G. B., Franz, H. S., & Vieira, B. M. (2023). Water Quality Indexes and Multivariate Statistic Methods Application: Case Study of Mirin Lagoon. Water, Air, & Soil Pollution, 234(12), 742. https://doi.org/10.1007/s11270-023-06746-2

[5] Municipalidad de Chile Chico & INGEOP. (2015b). Plan de Desarrollo Comunal de Chile Chico 2015-2018. Retrieved November 30, 2023, from https://www.chilechico.cl/archivador/pladeco1_2.pdf

[6] Salas Contreras, J. F. (2004). Diagnóstico y Clasificación de la Calidad de Agua en la Cuenca Del Río Baker según Objetivos de Calidad [Thesis]. University of Chile.

[7] Mol, J. H., De Mérona, B., Ouboter, P. E., & Sahdew, S. (2007). The fish fauna of Brokopondo Reservoir, Suriname, during 40 years of impoundment. Neotropical Ichthyology, 5(3), 351–368. https://doi.org/10.1590/s1679-62252007000300015

[8] White, C. (2012). Brownsberg Nature Park Situation Analysis 2012. WWF. Retrieved December 4, 2023, from https://wwflac.awsassets.panda.org/downloads/2012_04__brownsberg_nature_park_situation_analysis_white.pdf

[9] Berrenstein, H. J., & Gompers-Small, M. (Eds.). (2016). Second National Communication to the United Nations Framework Convention on Climate Change. Office of the President of the Republic of Suriname. Retrieved December 4, 2023, from https://unfccc.int/sites/default/files/resource/Surnc2rev.pdf

[10] Ministerio de Ambiente y Desarrollo Sustentable Presidencia de la Nación de Argentina & Inventario Nacional de Glaciares – CONICET. (2018). Informe de la subcuenca del Lago Viedma Cuenca del río Santa Cruz Parque Nacional Los Glaciares. In https://www.glaciaresargentinos.gob.ar/. Retrieved December 1, 2023, from https://www.glaciaresargentinos.gob.ar/wp-content/uploads/provincias/Santa_Cruz/docs/informes/informe_final_lago-viedma_APN_09-05-2018.pdf

Lake name / Location	Type	Area [Km²]	Avg. depth [m]	Trophic status	Ecosystem services	Lake uses
Titicaca / Bolivia and Peru	Lake	7,432	112	Mesotrophic	• Source of Water and Food • Microclimate Influence • Biodiversity Conservation • Cultural and Spiritual Significance • Transboundary basin • Recognition as a Ramsar Site [1]	Domestic, irrigation, hydropower [2]
Mirim / Brazil and Uruguay	Lagoon	4,199	6	Eutrophic	• Economic Importance • Source of Water and Food • Transboundary Basin [3]	Rice farming, recreation, water supply, navigation, fishing [4]
Buenos Aires / Argentina and Chile	Lake	1,855	400	Ultra-Oligotrophic	• Protected Areas, Wildlife Biodiversity [5] • Source of Water and Food • Economic importance [6]	Irrigation, drinking water, tourism, fishing, Transportation [6]
Brokopondo Reservoir / Suriname	Reservoir	1,135	21	Mesotrophic	• Biodiversity Impact [7] • Community Relocation and Cultural Impact [8] • Economy Importance [9]	Hydroelectric power, tourism, irrigation [8,9]
Viedma / Argentina	Lake	1,239	100	Oligotrophic	• Economic Importance [10] • Unique biodiversity [11]	Tourism, water supply [10]
Cerros Colorados Complex / Argentina	Reservoir	590	8	Mesotrophic	• Biological Diversity • Wildlife Refuge and Endemic Species [12] • Water Storage [13]	Irrigation, domestic supply, industrial, hydroelectric power [13,14]
Musters / Argentina	Lake	437	14	Mesotrophic	• Biodiversity Conservation • Economic Importance [15]	Irrigation, fishing and nautical sports [15]
Rogaguado / Bolivia	Lake	316	8	Eutrophic	• Refuge for biodiversity • Important breeding ground • Climate regulator • Source of freshwater [16]	Domestic supply, irrigation, fishing, tourism [16]
Villarrica / Chile	Lake	176	49	Mesotrophic	• Conservation Areas and Wildlife Preservation [17] • Economic Importance [18]	Aquaculture, hydroelectric energy, tourism [17,18]
Castillos / Uruguay	Lagoon	72	2	Eutrophic	• Unique Geographical Features • Biodiversity and Conservation	Forestry, agriculture,

[11] Administración de Parques Nacionales de Argentina. (2018). Plan de Acción para la Conservación Del Huemul en el PN Los Glaciares. Retrieved November 30, 2023, from https://www.cms.int/sites/default/files/document/Plan%20Huemul%20PN%20Los%20Glaciares_2019.pdf

[12] La Ciudad Posible. (n.d.). Cerros colorados, Reserva de Vida Salvaje. Cerros Colorados. Retrieved December 1, 2023, from https://www.cerroscolorados.com/

[13] Duke Energy Argentina. (n.d.). Centrales - Complejo Cerros Colorados. Retrieved December 1, 2023, from https://web.archive.org/web/20060902221909/http://www.duke-energy.com.ar/ES/Centrales/cerros_colorados.asp?id=1_2

[14] Emprendimiento Hidroeléctricos S.E.P. (2013). Apuntes sobre el Aprovechamiento Multipropósito Chihuido I. Retrieved December 1, 2023, from https://emhidro.com.ar/PDF/Apuntes_Chihuidol_esp.pdf

[15] Tejedo, A. & Instituto de Geología y Recursos Minerales de Argentina. (2004). Degradación de Suelos en los Alrededor es del Lago Colhué-Huapí. Retrieved December 1, 2023, from http://repositorio.segemar.gov.ar/308849217/1864

[16] Viceministerio de Recursos Hidricos y Riego de Bolivia. (2015). Plan Nacional de Cuencas de Bolivia. Retrieved December 2, 2023, from https://www.researchgate.net/publication/281244646_Plan_Nacional_de_Cuencas_de_Bolivia

[17] Instituto Nacional de Ecología y Cambio Climático de México. (2017). Evaluación de Servicios Ecosistémicos y de Riesgos por Cambio Climático en Cuencas Hidrográficas de Chile y México. Retrieved December 2, 2023, from https://www.gob.mx/cms/uploads/attachment/file/294880/CGACC_2017_Evaluacion_de_servicios_ecosistemicos_y_de_riesgos_por_cambio_climatico_en_cuencas_hidrograficas_de_Chile_y_Mexico.pdf

[18] Municipalidad de Pucón, DAOMA. (2019). Catastro de Humedales Urbanos y Rurales, Comuna de Pucón. Retrieved December 2, 2023, from https://www.municipalidadpucon.cl/oldweb/web2010/para%20descarga/ambiental/CatastroHumedalesPuc%C3%B3n2019.pdf

[19] Fundación Lagunas Costeras. (2023, March 4). Laguna de Castillos. Lagunas Costeras. Retrieved December 2, 2023, from https://lagunascosteras.org.uy/en/laguna-de-castillos-eng

					• Protected Landscape • Economic activities [19]	artisanal fishing, ecotourism and recreational activities [19]

To analyse meteo-climatic (i.e., air temperature and precipitation) and physical and water quality (LSWT, Chl-a, turbidity) trends we used Theil-Sen Test analysis (Carslaw and Ropkins 2012, R package *openair*). The period investigated was 1997-2020 for LSWT and 2003-2020 for Chl-a and turbidity. In the data preprocessing for Chl-a and turbidity variables a threshold of 20% of the number of pixels in relation to the maximum for the lake was set to avoid poorly observed datums where noise is more apparent. For the LSWT data of the Brokopondo Reservoir (GLWD00000106), the quality flag was extended to quality level 3 due to the low number of data available in the highest quality classes. Theil-Sen non-parametric test was used to assess the significance of the estimated median slope. The test results are for observed data, de-seasonalised, annual and seasonal data (December January February -DJF; March April May -MAM; June July August -JJA; September October November -SON).

The results from the Theil-Sen analysis both for de-seasonal and seasonal trends in the 10 selected lakes are reported in Figure 12.

Results of deseasonalised trends in Figure 12 show that Chl-a and turbidity increased in six and four lakes, respectively, when Theil-Sen trends were significant. Air temperature increased significantly in all but one lake, and LSWT significantly increased in three lakes while for the rest the change was not significant. Precipitation had a significant increase in two lakes.

The IPCC report (Castellanos et al. 2022) referred that warming has been detected throughout South America, except for a cooling trend reported for the ocean off the Chilean coast. In contrast, rainfall changes in South America vary geographically, with increasing trends in precipitation particularly observed in the Southeastern sub-region and decreasing trends in the Southwestern sub-region.

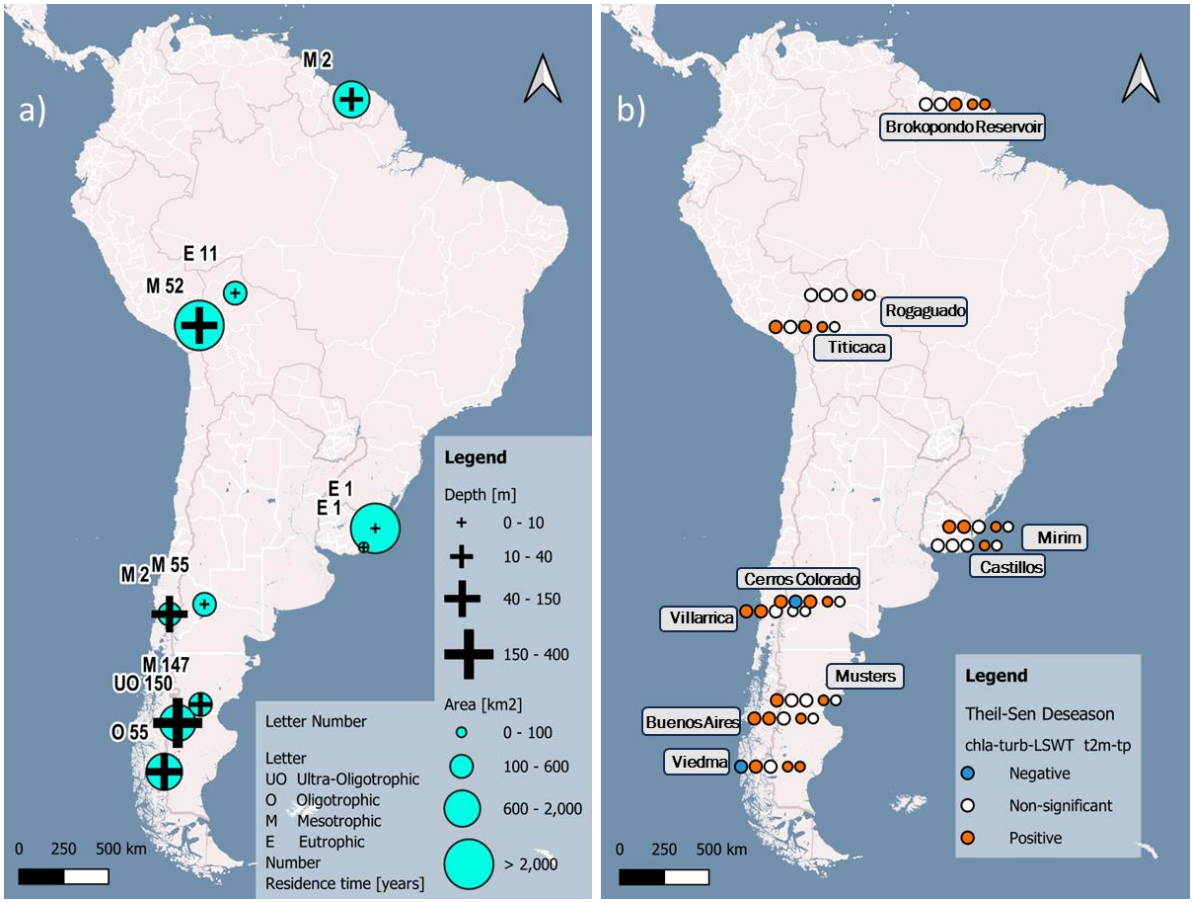

Figure 12. South American lakes with (a) depth, trophic status, residence time and area information and (b) results from the Theil-Sen analysis with, displayed as dots from left to right, deseasonalised trends in Chl-a, turbidity, LSWT, air temperature (t2m) and total precipitation (tp).

Results of seasonal trends of Chl-a in Figure 13 (left panel) show varied responses for different seasons in the ten lakes. Chl-a increased in all seasons only in Lake Titicaca (GLWD00000020, mesotrophic) and Lake Mirim (GLWD00000046, eutrophic lagoon). In two lakes (at the latitudinal extremes), Chl-a decreased in December - February (DJF): Lake Brokopondo (GLWD00000106, mesotrophic) in Suriname at 4.7°S latitude, and Lake Viedma (GLWD00000171, oligotrophic) in Patagonia at –49.6°S latitude.

Where turbidity showed a significant seasonal trend as shown in Figure 13Figure 12 (centre panel), it usually increased all year round or in the March - May (MAM) season. The exception was Lake Cerros Colorados (GLWD00000379) in Argentina, a reservoir belonging to a group of basins with dams and hydroelectricity generation facilities, which had decreasing trends of turbidity across all seasons.

For LSWT, trends are shown based on lake latitude, in accordance with the State of the Climate report 2022 (Carrea et al. 2023b). For lakes at latitudes < -23.5, the summer (DJF) Theil-Sen trend is shown, while for lakes at latitude between -23.5 and 23.5 the deseasonalised trend is reported (Figure 13, right panel).

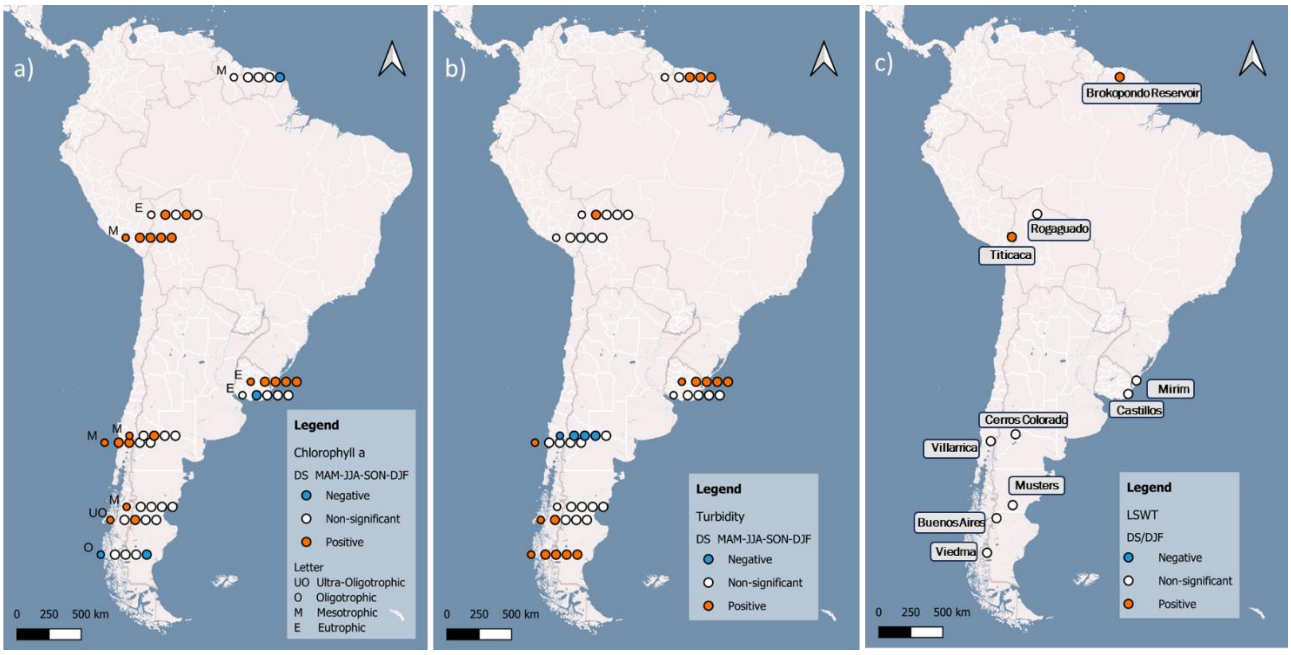

Figure 13. Map of results from the Theil-Sen analysis with deseasonal (DS) and seasonal trends in chlorophyll-a (a), Turbidity (b) and lakes surface water temperature (LSWT; c) in the 10 South American selected lakes. In panel b) dots from left to right: MAM=March-April-May; JJA=June-July-August; SON=September-October-November; DJF=December-January-February. For LSWT the trend is reported for DJF at latitudes < -23.5 and deseasonalised for the (sub)tropical region.

6.1.1.2 Heatwaves and lake temperature anomalies

The above analysis provides a first overview of temporal trends. Additional investigations included heatwaves and temperature anomalies as indicators of climate change effects, as developed in Use Case 3 of this report. The heatwave indicator assesses extreme temperature events in lake water (LSWT) and is defined when lake water median temperature exceeds the seasonal 90th percentile of the entire time series and persists for at least two consecutive days within a five-day period (Hobday et al. 2016, Woolway et al. 2021). The temperature anomalies indicator is calculated on the LSWT data of quality levels 4 and 5 to ensure data reliability. De-seasonalised lake median of time series for the five warmest months of the year was used based on historical climatology.

Lakes located south of -32° latitude were the most affected by prolonged heatwaves, particularly in the year 2008. For instance, in March 2008 a heatwave hit Lake Musters (GLWD00000448, Argentina) for 21 days and lake Buenos Aires (GLWD00000094, Argentina and Chile) for nine days, and Lake Villarica (GLWD00001109, Chile) was hit by a heatwave in February 2008 for 11 continuous days. Lake Viedma (GWLD00000171) also experienced the 2008 heatwaves, although for only two days while a successive heatwave event occurred in 2013.

Lakes of the extreme southern sub-region of South America (<-45.0°S) experienced several positive LSWT anomalies. In particular, the two large deep lakes located along the Andean region, Lake Viedma (GLWD00000171) and Lake Buenos Aires (GLWD00000094) experienced continuous positive LSWT anomalies during the entire time series investigated (Figure 14). For Lake Viedma the largest positive anomalies were recorded in 2008 and 2013 (> +1.2°C) and heatwave occurrence was recorded three times, the longest at four days in April 2013. For Lake Buenos Aires the largest positive anomalies were recorded in 2008 and 2009 (> +1.6°C), corresponding to the longest heatwave occurrences of nine and seven days during 2008. In this lake, heatwaves were often recorded. In lake Musters (GLWD00000448),

located in the same region, the highest LSWT anomalies (> +1.5 °C) were registered in 2008 and 2013, when also the most prolonged heatwaves occurred (of 21 and 13 days, respectively).

Furthermore, in Lake Villarica (GLWD00001109, -39.2 °S) and the Cerros Colorados reservoirs (GLWD0000379, - 38.5 °S) located at similar latitude, less continuous but repeated events of positive LSWT anomalies were recorded in various years (Figure 15). In Lake Villarica the highest anomalies (<> +1.0 °C) were recorded in 2008, 2009 and 2013, when persistent heatwaves (9 - 11 days) also occurred, and in Cerros Colorados extreme LSWT anomalies were recorded in 2009 and 2013 (> +1.7 °C), with the longest heatwave recorded in 2013 for 11 days.

In the above-described lakes, the lowest and relatively continuous negative temperature anomalies, with values ranging between –0.9 °C and –2.3 °C, were recorded during the year 2010.

Lakes located at higher latitudes and on the east coast of South America include two shallow lagoons, Castillos (GLWD00002092) and Mirim (GLWD00000046) in Uruguay, which seemed to be affected by several but shorter heatwaves (< 3 days), with the exception of a 9-day heatwave hitting Castillos in 2015 (Figure 16). They both experienced several extended periods of water temperature anomalies, spanning a wide range between positive (max +2.0) and negative (min –2.4) values.

In the large and deep Lake Titicaca, (GLWD00000020, -15.9 °S) located in the Andean highlands at 3,812 m, the range of LSWT anomalies appeared more restricted than for other lakes, likely due to the buffer effect of the large volume of lake water and to the presence of strong winds. Positive anomalies appeared consistent during 2005, 2010 and 2016 although always with moderate values (between +0.5 °C and +0.7 °C), except for a higher anomaly (> +1.0 °C) in 2016 when also the only heatwave was recorded in the lake (Figure 16).

For the remaining lakes of our study, the data available were too scarce to calculate reliable temperature anomalies and heatwaves.

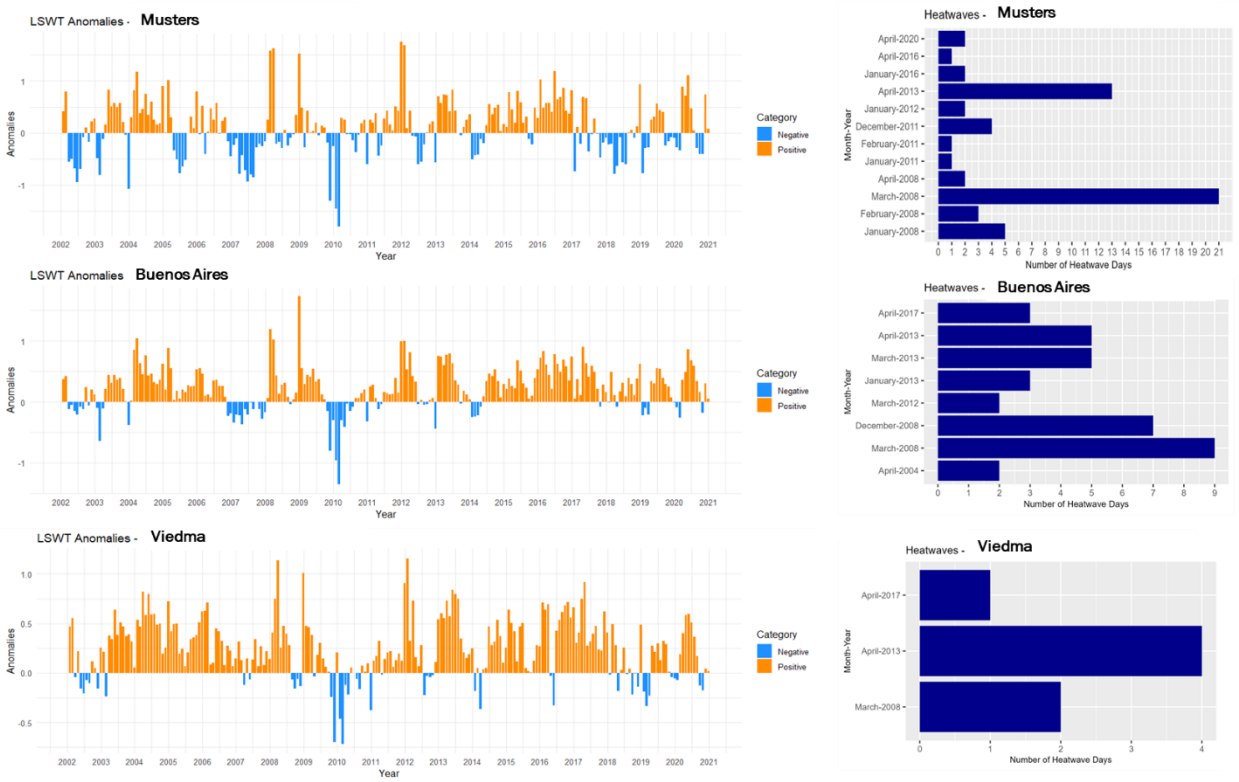

Figure 14.Lake surface water temperature (LSWT) anomaly indicator (left) and Heatwave occurrence indicator (right) for the Lake Musters, Lake Buenos Aires, and Viedma Lake.

Figure 15. Lake surface water temperature (LSWT) anomaly indicator (left) and Heatwave occurrence indicator (right) for the Cerros Colorado Complex and Villarrica Lake.

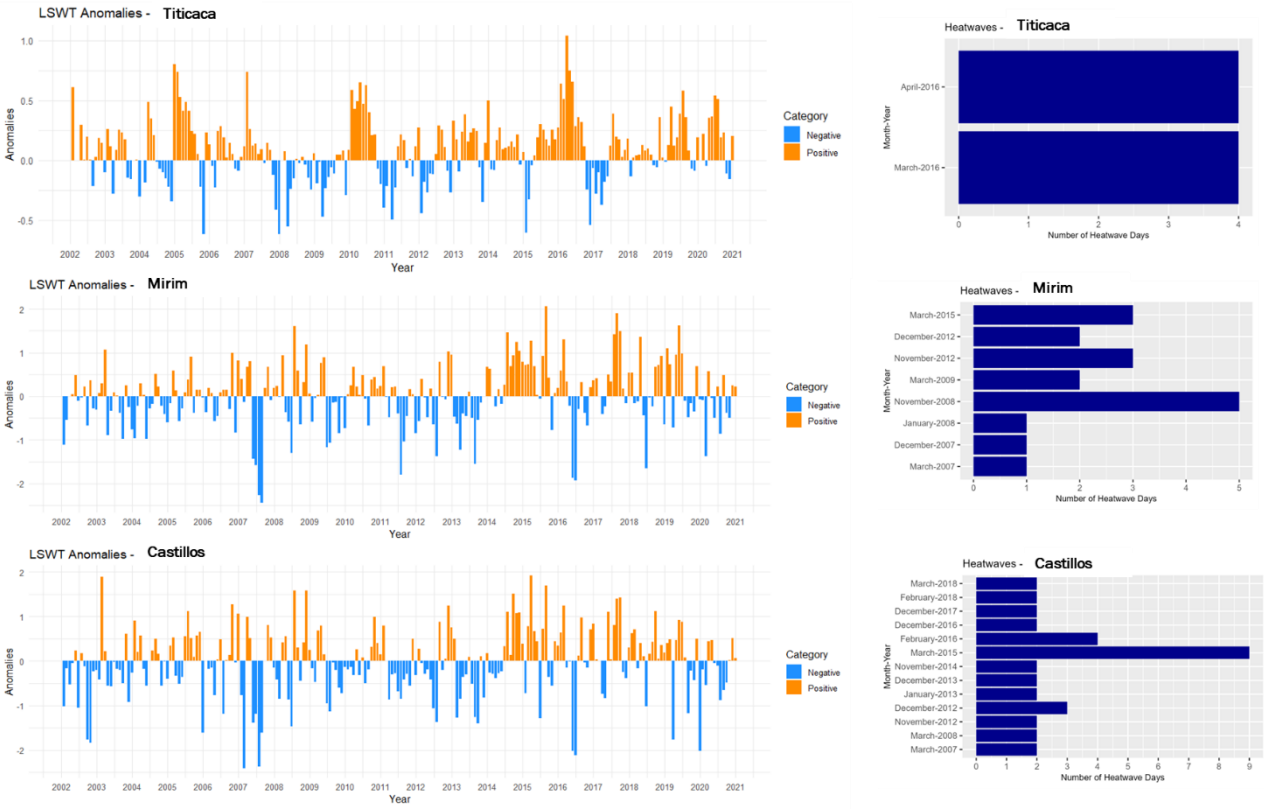

Figure 16. Lake surface water temperature (LSWT) anomaly indicator (left) and Heatwave occurrence indicator (right) for Lake Titicaca, Mirim Lagoon and Castillos Lagoon.

The above analysis represents a first overview of temporal trends in lake parameters and climatic indicators for the selected South American lakes. Future investigations include spatial trend analysis of singular lakes and exploration of potential changes in Chl-a, as proxy of phytoplankton community temporal shifts due to climatic changes (Lizana, 2023).

7 Global scale assessment

7.1 Trends of water quality in shallow lakes

Shallow lakes represent a prominent part of inland waters, providing significant contributions to biodiversity and delivering many other ecosystem services. Because of their relatively larger surface-to-volume ratios, shallow lakes are susceptible to environmental changes (Feuchtmayr et al. 2009) and prone to switching from a clear-water, plant-dominated to a turbid water state dominated by suspended sediment or phytoplankton under eutrophication pressures (Scheffer et al., 1993). Having strong interactions between sediment and the overlying water, shallow lakes are also highly sensitive to climate change (Wilhelm and Adrian 2008) and tend to respond more directly to short-term weather variations like storms (Deng et al. 2018). Consequently, the depth of a shallow lake can be subject to strong fluctuations resulting from climatic variability with important potential impact of climatic extremes (floods or drought) on their hydrology and ecology.

Climate change is expected to have a large impact on shallow lakes, with warmer conditions having a large effect on lake ecosystems both in food web structure through the 'trophic cascade' from phytoplankton to fish (Scheffer and Van Nes 2007), and through changes in catchment hydrology and nutrient load to lakes (Straile 2002). Warming is also expected to enhance internal nutrient loading of shallow lakes through increased remineralization rates (Sondergaard et al. 2003, 2013).

We selected 352 shallow lakes of average depth ≤ 3 m (Moss et al. 2003). These are distributed in all continents, covering diverse climatic and ecological settings. Analyses of trends for LSWT, Chl-a and turbidity were carried out using Theil-Sen trend analysis (Carslaw and Ropkins 2012, R package *openair*) for the period 2002 - 2020.

For Chl-a, the Theil-Sen analysis was performed on 249 lakes with adequate data (free of large data gaps) and resulted in 165 lakes having a significant deseasonalised trend, of which 110 (67%) lakes had a positive trend and 55 (33%) lakes a negative trend in Chl-a (Figure 17).

Exploring seasonal trends in more detail shows that lakes at higher latitudes (>23.5°) in temperate and continental regions had a significant Chl-a increase, particularly in summer (JJA) and in autumn (SON) (65 % and 64 % of the lakes, respectively). This was in contrast to the winter (DJF) and spring (MAM) period when there were almost equal amounts of lakes having positive and negative Chl-a trends. Similar results appeared in lakes at lower latitudes (<23.5°), where Chl-a had a significant increase in winter (DJF) and spring (MAM), however with lower confidence because of the smaller number of lakes included in this climatic zone.

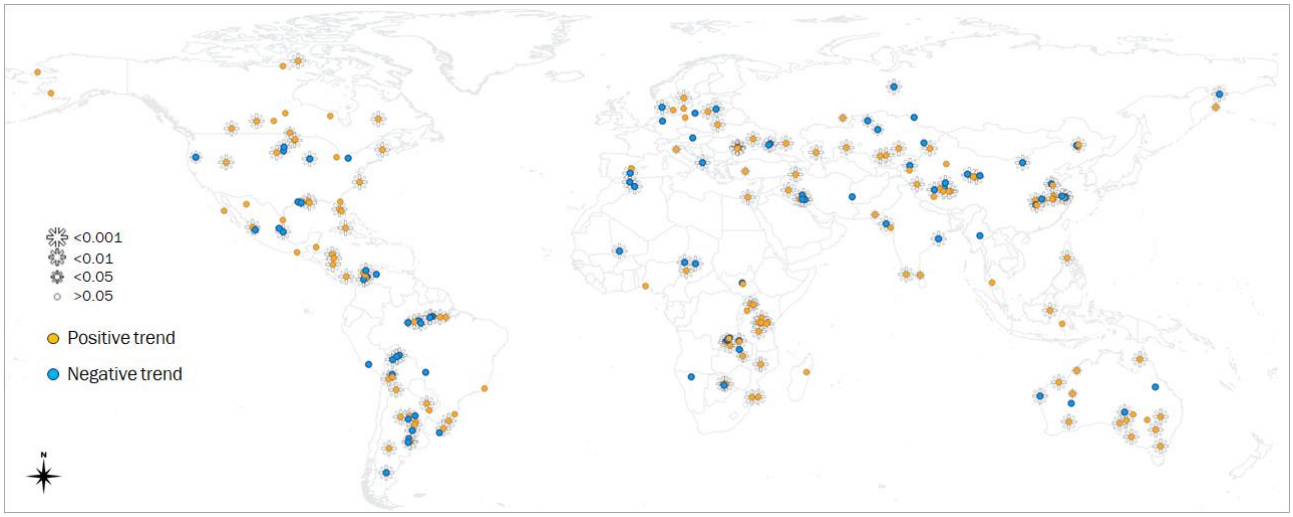

Figure 17. Map of distribution for Chl-a trends (orange=positive trend; blue=negative trend; overlaying star=significant trend) for CCI shallow lakes, during 2002-2020.

For turbidity, out of a total of 190 lakes with adequate data, 147 lakes had a significant deseasonalised trend, of which 114 (78%) were positive and 33 (22%) were negative (Figure 18). Exploring seasonal trends further shows globally higher percentages of lakes with increasing turbidity trends in DJF and MAM seasons, especially in the southern part of the globe (latitude < -23.5°).

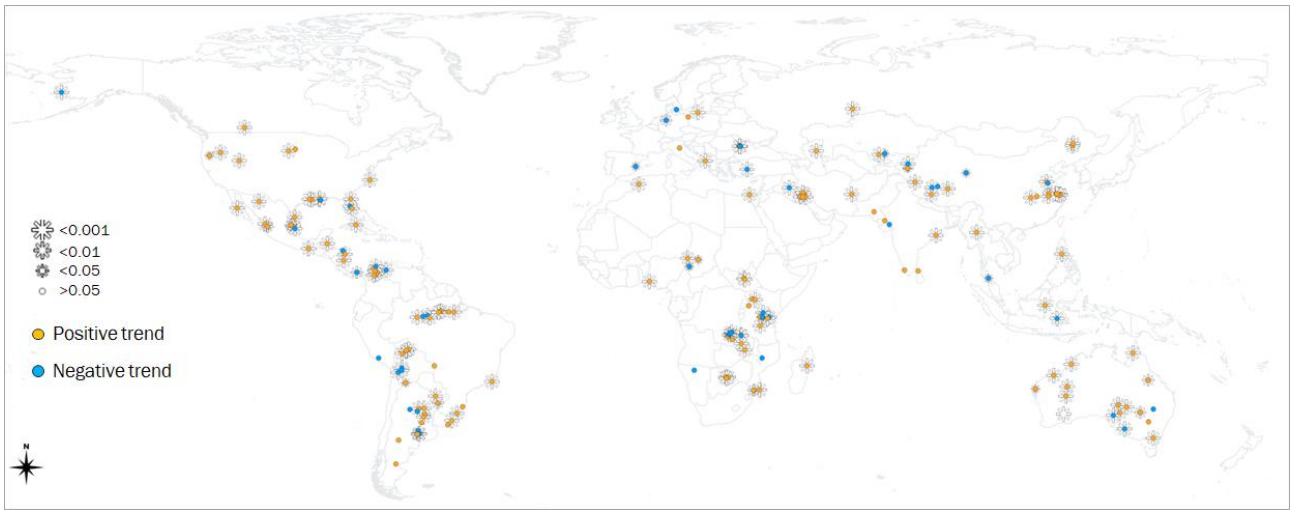

Figure 18. Map of distribution for turbidity trends (orange=positive trend; blue=negative trend; overlaying star=significant trend) for CCI shallow lakes, during the period 2002-2020.

For LSWT we selected summertime data as July - September at latitudes >23.5°, and December - February at latitudes <-23.5°. Between these latitudes the entire year was used, as in Carrea *et al.* (2023b). Starting from a total of 206 lakes, only 66 show a significant trend in the Theil-Sen analysis. Significant trends in LSWT appear more frequent for lakes in the tropical belt and in the southern hemisphere (Figure 19).

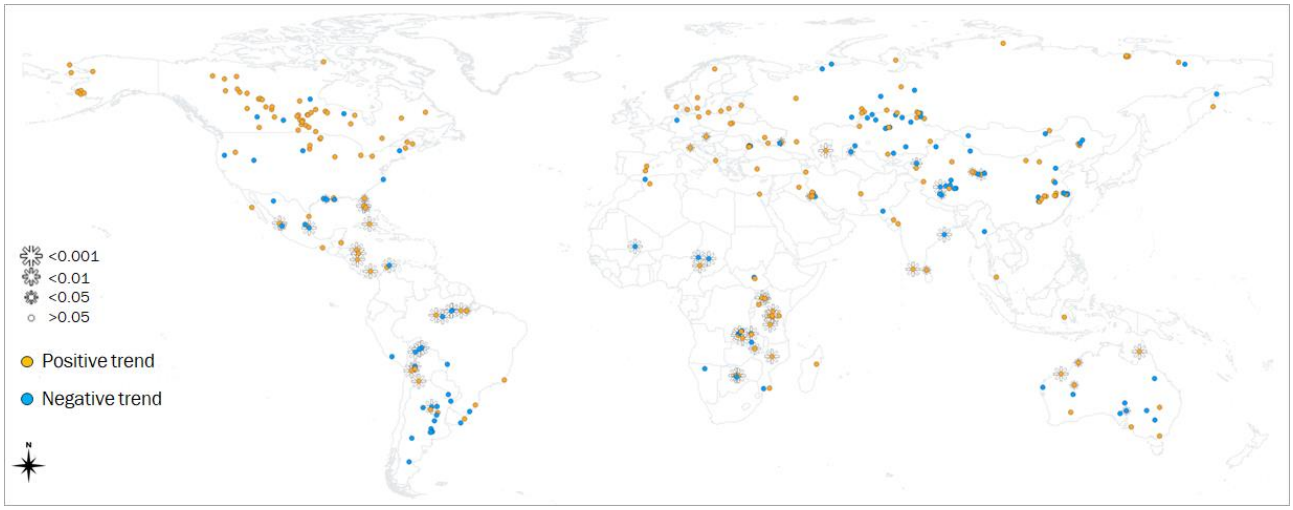

Figure 19. Map of distribution for LSWT trends (orange=positive trend; blue=negative trend; overlaying star=significant trend) for shallow lakes, during 2002-2020.

The results of our study suggest that, worldwide, shallow lakes are getting more turbid and with increasing Chl-a, as proxy of phytoplankton biomass. Climate change can play a part in this process, with warmer temperatures affecting food web structures and ecosystem functioning of shallow lakes, and climate driven changes in precipitation affecting catchment hydrology, nutrient inputs and internal processes in lakes. To disentangle the effects of climate change from other human-induced influences, which impact lake catchments by changes in land-use and in nutrient inputs (and consequently affecting lake water quality of shallow lakes), is a challenging task. Future work will include testing for interannual associations between Chl-a, turbidity and LSWT, comparing across lakes to investigate their geographical, morphometric and ecological characteristics. Furthermore, specific lake case studies with in-situ monitoring data may help to validate these findings and further investigate the interactive effects of temperature and nutrients on lake water quality.

7.2 Meteorological factors influencing LSWT across different climates

LSWT prediction has received considerable attention in the last decade, due to a need to observe trends of global warming and its effect on lakes and vertical mixing. For such predictions, a number of atmospheric variables must be considered, depending on the modelling strategy adopted. The two main modelling strategies are physics-based versus data-driven modelling.

Physics-based models use fundamental equations of lake heat budget and, depending on model complexity, may require information on lake morphology, inflows and outflows, in addition to meteorological variables (Piotrowski and Napiorkowski 2018), to properly describe the 1-to-3D physical processes determining LSWT.

Data-driven models only depend on the observed LSWT and meteorological variables and do not use detailed knowledge of the physics of lakes. Machine learning (ML) approaches are commonly adopted for global-scale studies, as they are more flexible than physically based models and allow removing or changing predictors (in our case meteorological variables) for interpreting the variability of the outputs (LSWT). The combination of these two modelling strategies, hybrid modelling, benefits from both approaches and has raised substantial success in the last decade (e.g. air2water, Piccolroaz et al. 2013, Toffolon et al. 2014).

Among the many ML approaches used to predict LSWT we find multiple regression models, based on linear relationships (Sharma et al., 2008), random forest (Heddam et al. 2020; Zhu et al. 2020), support vector machine (SVM, Quan et al. 2020), artificial neural network (ANN, Sharma et al. 2008; Sener et al. 2012; Read et al. 2019; Zhu et al. 2020a,b).

As predictors of LSWT, the most common meteorological variables are air temperature (AT), wind speed (WS), shortwave (SWR) and longwave (LWR) radiation, relative (or specific) humidity (RH), rainfall (R), water depth and air pressure (AP). Among these, AT has been confirmed as the most influential indicator by many studies (Sharma et al. 2008; Sener et al.2012, Read et al. 2019, Heddam et al. 2020, Zhu et al. 2020b). In addition to AT, the day of the year (DOY) has shown a positive impact on the LSWT prediction, especially if formulated as sine and cosine of DOY (SDOY, CDOY, Yousefi and Toffolon 2022). The LSWT is either obtained from in situ measurement or remote sensing, while meteorological variables are generally derived from weather stations or globally available models.

In this study (Yousefi pers comm., Yousefi et al. *in prep*) we evaluate the influence of meteorological variables on LSWT in 2024 lakes from the Lakes_cci dataset using Back Propagation in Neural Network (BPNN) as a ML approach. We test the influence of eight meteorological variables from ERA5 dataset plus DOY and different combinations of them. We also investigate the accuracy of BPNN as a ML approach to predict LSWT when a limited number of valid observations are available.

Based on the Köppen climate classification (Köppen 1918), lakes are categorized into five distinct regions, each representing different climatic conditions: tropical, dry, temperate, snow and polar. To ensure the robustness and stability of the results, we ran the model 20 times and subsequently calculated the average of the obtained results. Model performance is assessed based on two performance metrics: the root mean square error (RMSE) and the modified Nash-Sutcliffe efficiency index (NSE*, Schaefli and Gupta 2007, Piccolroaz et al. 2016). The latter index considers the climatological year as a benchmark model and allows accounting for the seasonal variability of the target (LSWT). Finally, to include the lakes thermal inertia, we took the weighted average of the forcing variables over a specific time span preceding the day of LSWT acquisition. The optimal averaging window was determined based on BPNN model performance.

The performance of the test set of BPNN for all lakes shows good performance in both training and test experiments, with RMSE between 1.5 and 2°C globally (Figure 7.2.1). Such performance can be improved, despite it's not too far from other studies modeling LSWT globally (Piccolroaz et al. 2020).

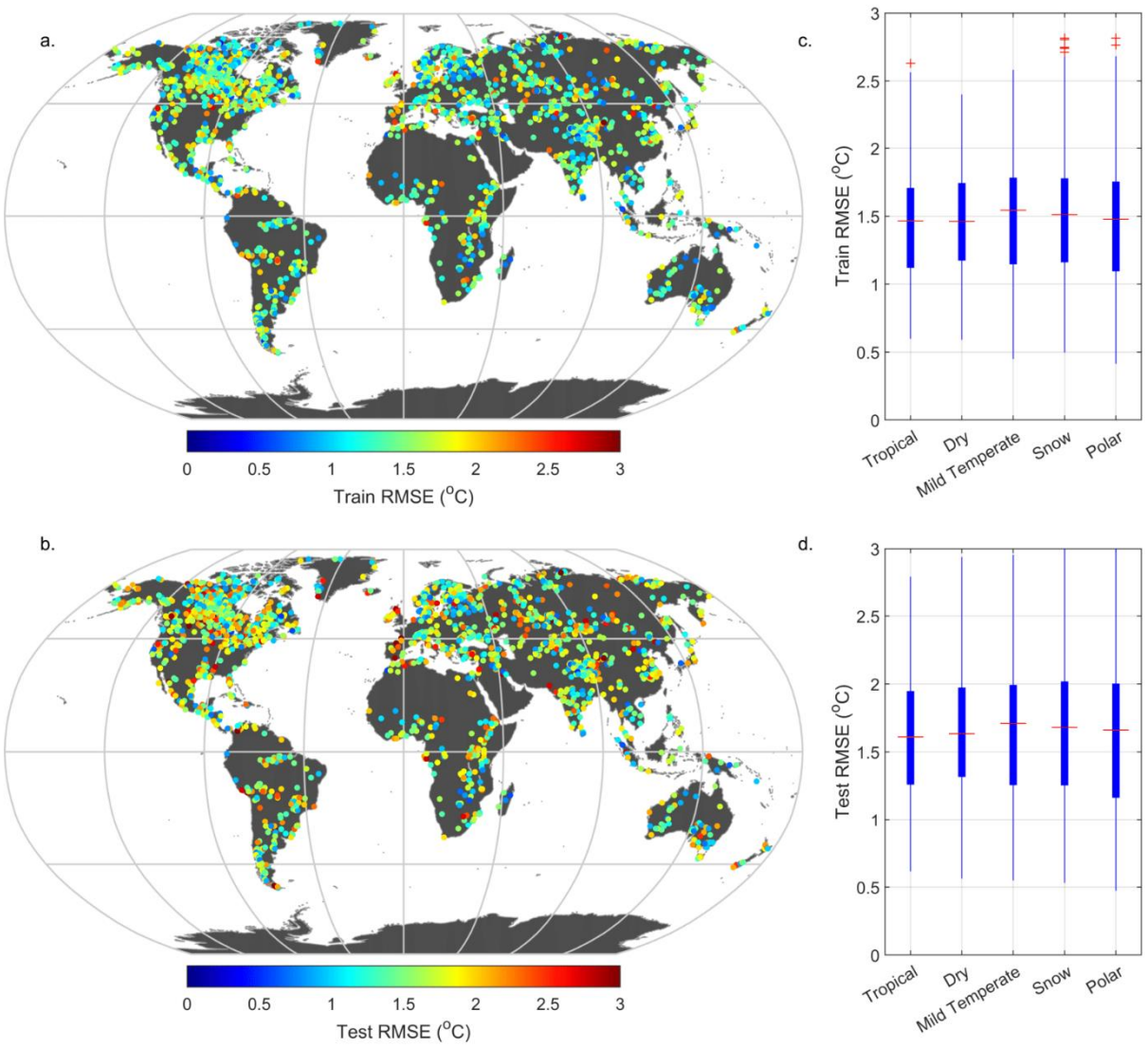

Figure 20. Performance of BPNN in all Lakes_cci in terms of RMSE in (a, c) training and (b, d) test sets for all Köppen regions (Source: Yousefi, 2023).

In all Köppen regions, the information on the DOY (SCDOY) appears to dominate the prediction of LSWT. If such information is excluded from the feature ranking model, then shortwave and longwave radiation are the most influential on LSWT variability (Figure 21). Air temperature appears to be the third most influential variable in all regions but in the Tropical region, where it is surpassed by relative humidity and rain. Further analysis will be conducted to estimate how the seasonal modulation of both our target and its predictors affects the feature ranking. In fact, the most influential variables across all regions (AT, LWR, SWR, RH) have significant correlations with SDOY and CDOY, and consequently among themselves.

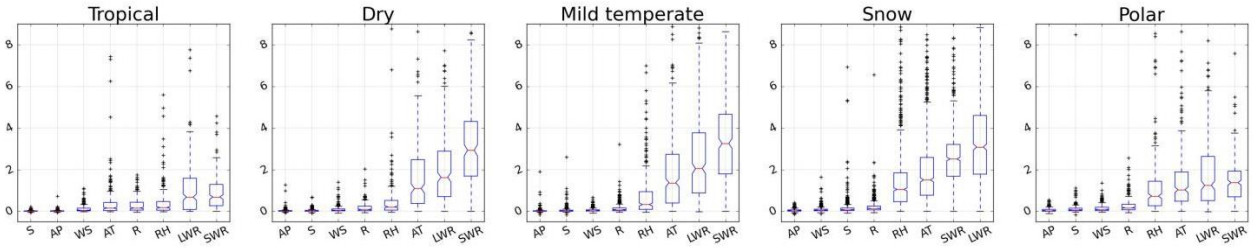

Figure 21. Feature ranking of meteorological variables in the Köppen regions (Source: Yousefi, 2023).

Our findings showcase the potential of the BPNN model to simulate and predict LSWT dynamics, and to identify the most influential climate variables. Our exploration of predictor rankings reinforces the idea that these variables hold significant influence, particularly in tropical regions. The main predictor, SCDOY, emerged as the primary driving factor behind LSWT variability. For deepening the comprehension of LSWT dynamics across different climates, further analysis will be conducted on anomalies of LSWT and atmospheric variables.

8 Use cases

8.1 Heatwave and storm event impacts on lakes (CNR)

According to model projections, increases in the duration, intensity, and spatial extent of heatwaves over most land regions are expected. In the context of climate change, the impact of extreme climate events, such as heatwaves, demonstrates the vulnerability of lake ecosystems to climate variability. In temperate lakes, fish die-offs occur more frequently in lakes of higher temperature and during periods of extreme heat and such events are predicted to double by mid-century with implications for species displacement, size spectrum or even depopulation (Till et al. 2019). The IPCC predict that warming is set to continue with an over 90% likelihood of a continuation of the increase in the frequency of heat extremes over the 21st century in Europe, especially in southern regions (Ranasinghe et al. 2021). Recent projections estimate that lakes will get warmer for longer periods, with heatwaves potentially spreading across multiple seasons (Woolway et al. 2021). In some regions, heatwaves can add to existing pressure from drought which can reduce lake levels and areal extent (both detectable from satellite images) resulting from reduced inflows, increased evaporation and extraction for anthropogenic purposes (Zhao et al. 2022). This can have significant implications for ecological functioning in lakes.

The trend toward a warmer, drier, and more extreme European climate has been underway for several decades. The increase in frequency of European heatwaves has been associated with the reduction in Arctic Sea ice and Eurasian snow cover and is likely to continue during the next century (Zhang et al. 2020). In the summer of 2019, a widespread double heatwave event occurred in Europe resulting in one of the top five warmest summers since 1500 (Sousa et al. 2020). We investigated responses of the 2019 European heatwave on 36 selected lakes (Figure 22) using Lakes_cci Chl-a estimates, and we assessed how the lake response varied depending on latitude and total phosphorous concentration.

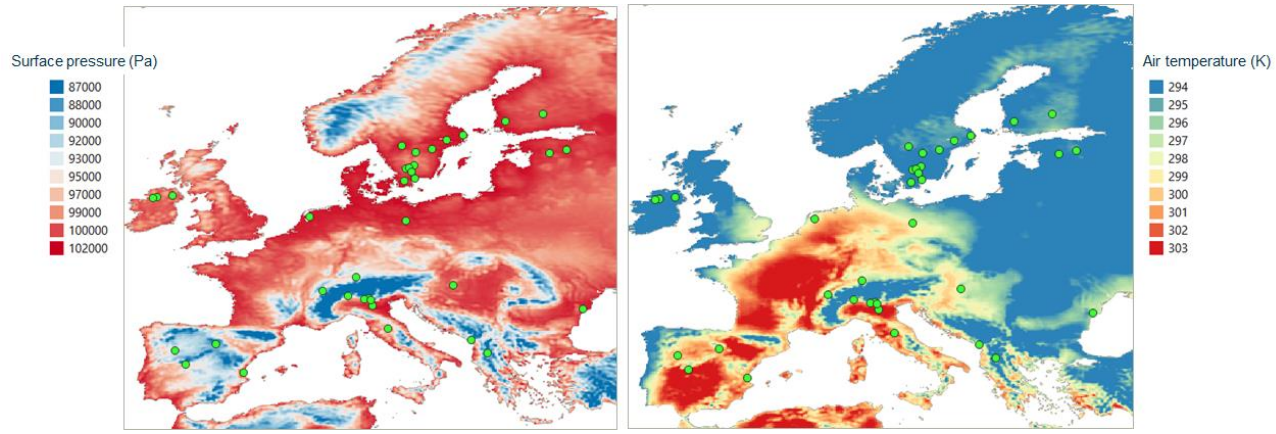

Figure 22. Map of Europe showing 36 lakes (green dots) together with (left) surface pressure (Pa) and (right) air temperature (K) on 24 July 2019. Data sourced from ERA5. Modified from Free et al. (2022).

For some shallow lakes (Figure 23), peak temperatures during a heatwave event appeared to coincide with a decline in Chl-a. For example, in Lake Võrtsjärv (Estonia), as temperature increased to 24 °C during the second heatwave, Chl-a declined from 36 (on DOY 186) to 16 mg m^{-3} (DOY 209) before increasing to 34 mg m^{-3} following the storm or low-pressure event that ended the heatwave (DOY 214). Similarly, in lake Trasimeno (Italy), larger increases in Chl-a corresponded to low-pressure events at the end of the heatwave, increasing from 12 (on DOY 206) to 15 mg m^{-3} (DOY 214). In contrast, for lake Bolmen (Sweden) results were more variable and a pattern less clear.

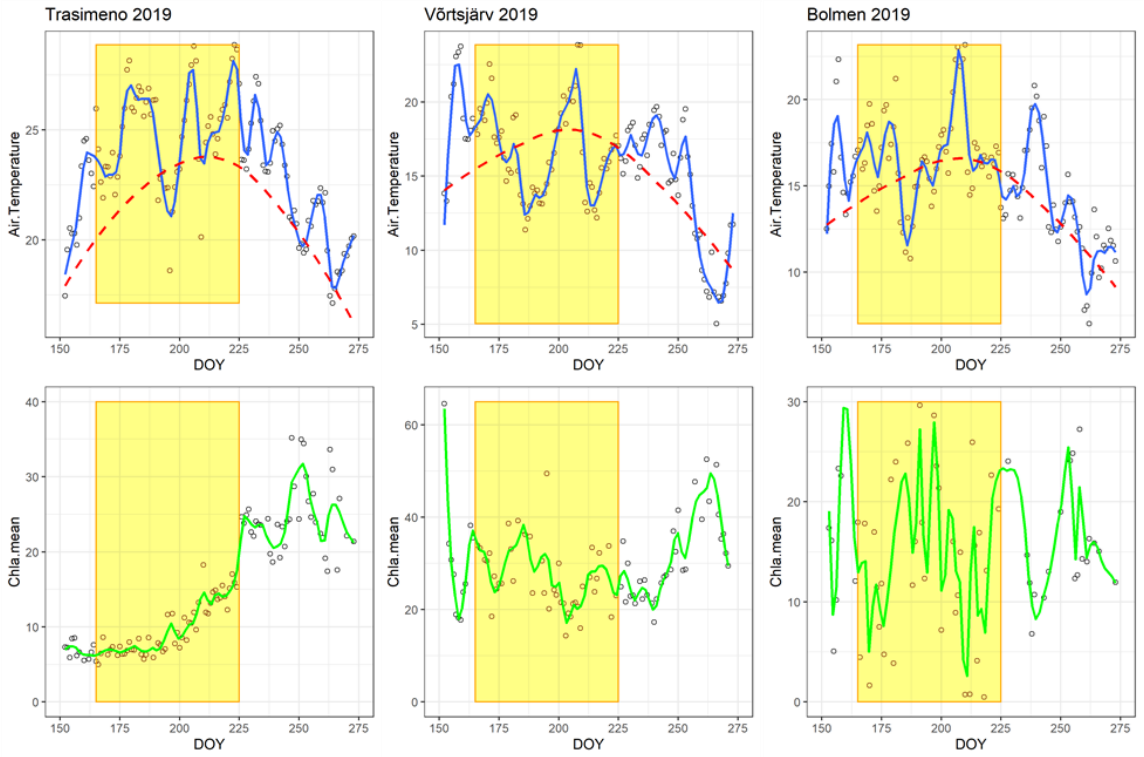

Figure 23. Response of three shallow lakes to the double heatwave event. From left to right: Trasimeno (Italy), Võrtsjärv (Estonia), Bolmen (Sweden). (Top) daily air temperature in 2019 (dots with blue smoothed lowess line) and average air temperature (◦C) during 1981-2010 (red dashed smoothed lowess line). (Bottom) Mean lake Chl-a concentration in 2019 (dots with green smoothed lowess line). Yellow box highlights day of year (DOY) between 165-225 (14 June - 13 August). Source: Free et al. (2022).

In deeper lakes of the Alpine region (Maggiore, Constance and Garda), generally in nutrient poor conditions, Chl-a was always relatively low, although an increase was visible in synchrony with rising temperatures in the first but not the second heatwave (Figure 24).

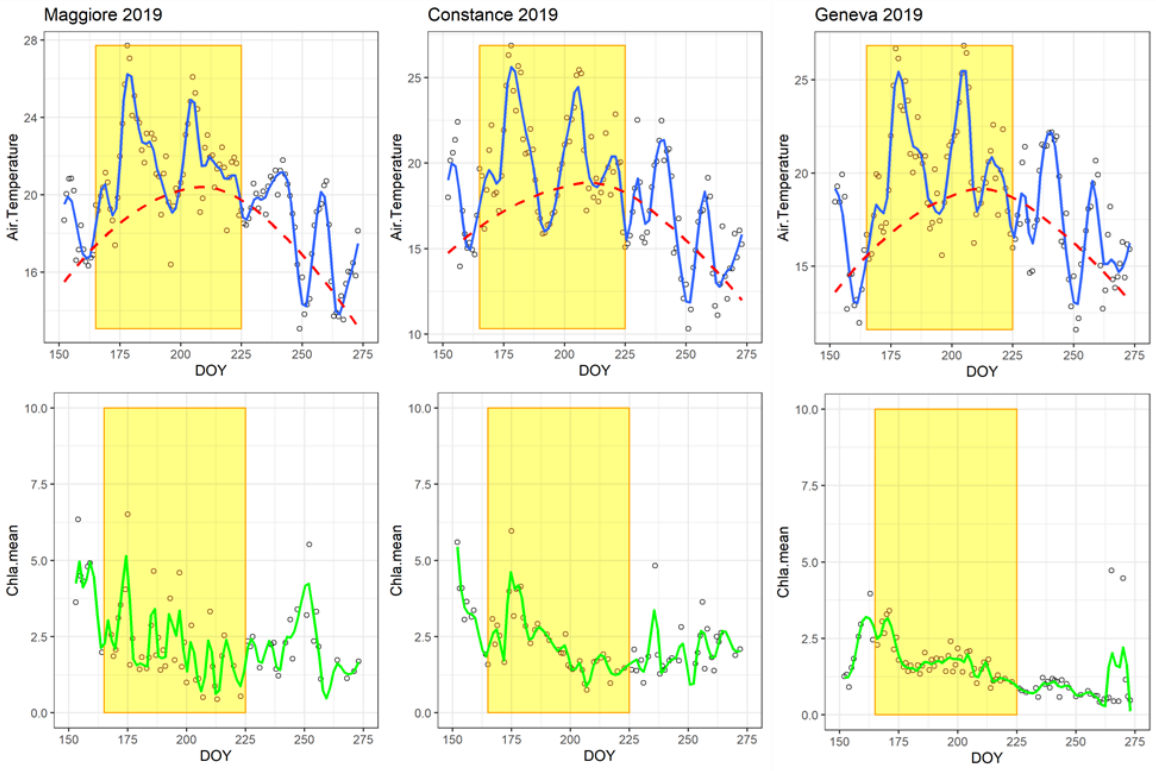

Figure 24. Response of three deep Alpine lakes to the double heatwave event. From left to right: Maggiore (Italy), Constance (Germany/Switzerland), Geneva (France/Switzerland). (Top) Daily air temperature in 2019 (dots with blue smoothed lowess line) and average air temperature (◦C) in 1981-2010 (red dashed smoothed lowess line). (Bottom) Mean lake Chl-a concentration in 2019 (dots with green smoothed lowess line). Yellow box highlights day of year (DOY) during 165-225 (14 June-13 August). Source: Free et al. (2022).

The study, detailed in Free et al. (2022), concluded that the timing and magnitude of the response to the heatwave events depends on lake depth (Figure 25) and nutrients. Deeper lakes respond sooner, probably because of higher temperatures leading to stronger stratification, thereby improving the light climate but with the response strength dependent on nutrient status. This was supported by lakes at higher latitudes, typically colder, showing greater synchrony between air temperature and Chl-a. In contrast, shallower lakes, not typically light limited, and lakes at lower latitudes shown more asynchrony – with a greater response after the heatwave event probably as a result of internal and external loading. The phenology of the phytoplankton relative to the heatwave event is likely to be of key importance as several shallow lakes had much larger blooms outside the heatwave period, during late summer and early autumn. Using remote sensing to derive estimates of Chl-a as an indicator of phytoplankton abundance is the most feasible method of providing key data that is both at high frequency and synoptic – capable of covering large scale weather events at continental scale.

Following on from these conclusions by Free et al. (2022), further work investigated the responses of lake water quality to rising temperatures during heatwaves and to low-pressure events at the end of heatwaves in other continents.

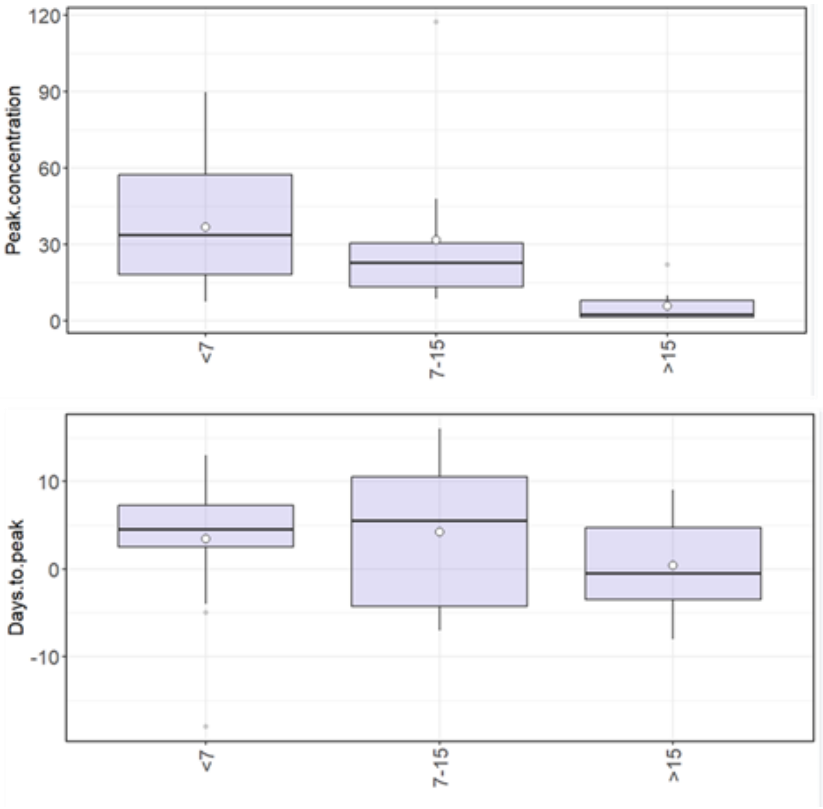

Figure 25. Timing (days) and concentration (mg m^{-3}) of peak in Chl-a with respect to the second 2019 heatwave for the three depth lake groups (<7m; 7-15m;>15m).

8.2 La Niña influence on water quantity and quality of a reservoir in a hot desert climate (Lake Qadisiyah, Iraq) (UoS)

Lake Qadisiyah is located on the Euphrates River and has a surface area of 461 km^2. Its catchment covers part of Turkey, Syria and Iraq, inflow water of this lake is mainly from snowmelt and precipitation. Lake Qadisiyah provides important water resources for irrigation and hydroelectricity production. Because of the semi-arid climate, water resources are extremely valuable, and the availability of water in this lake is sensitive to both climate change and human activities. We look at this lake as a pilot study on the drivers of water quantity and quality changes including climate and other anthropogenetic factors.

We used LWL, Chl-a, and turbidity products from the Lakes_cci dataset covering the period of 2000–2019, first looking at water level and water quality changes in the past 20 years, and their relationship. In addition, we collected precipitation, wind speed and air temperature data in the lake catchment for 2000-2019 from the ECMWF ERA 5 dataset, the standardized precipitation index (SPI) expressing drought in the lake catchment for 2000-2019 from Copernicus Emergency Management Service, and the bi-monthly El Niño/Southern Oscillation (MEI) data from National Oceanic and Atmospheric Administration (NOAA). Those data were used to investigate causes of water quantity and water quality changes in the lake.

There have been four periods when water level was clearly and continuously lower than the average of the studied 20 years (138.3 m, Figure 26): September 2000 to December 2001, August 2008 to December 2011, November 2014 to March 2016, and August 2017 to February 2019. Chl-a

concentration and turbidity were clearly elevated when water level was low in the periods 2008-2011 and 2017-2019 (Figure 26).

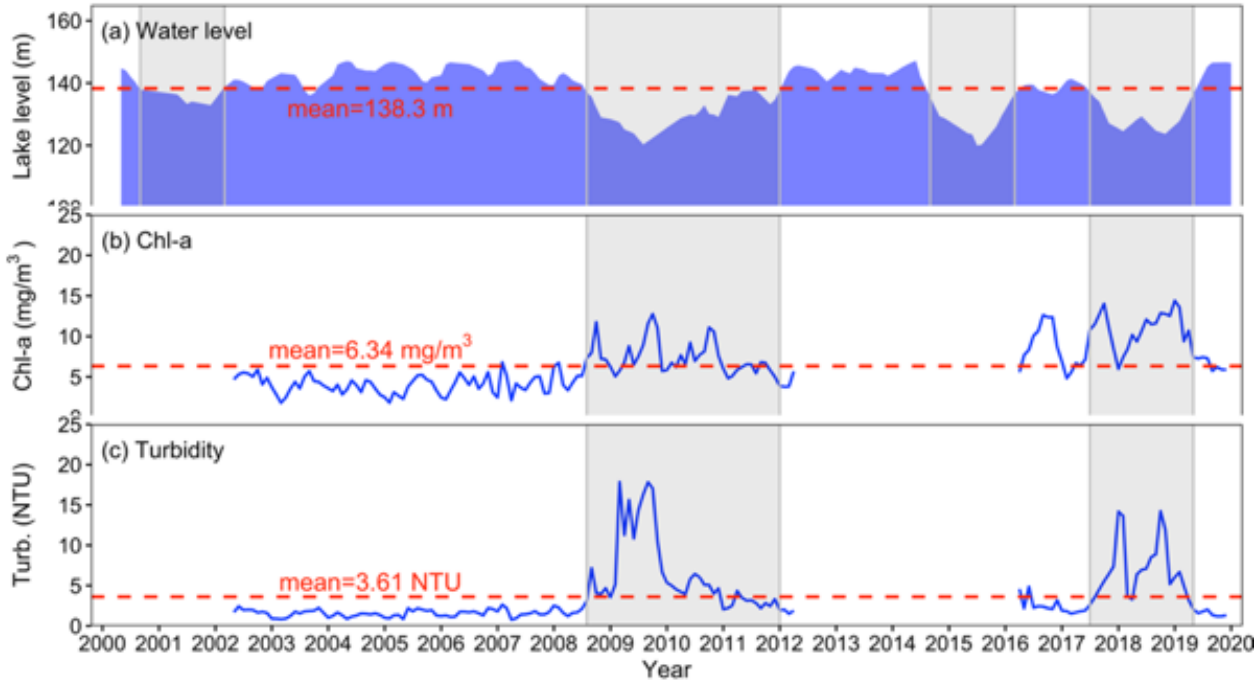

Figure 26. (a) Water level, (b) Chlorophyll-a, and (c) turbidity during 2000 - 2019 in Lake Qadisiyah.

The spatial distribution of yearly average Chl-a concentration is shown in Figure 27. Chl-a concentration in the river inflow regions (west part of the lake) is higher than in the lake centre (east part of the lake). Chlorophyll-a concentration in 2008 - 2011 and 2016 - 2019 were higher than in other years. The observed lake area in 2008, 2009, and 2018 was also clearly smaller compared to other years.

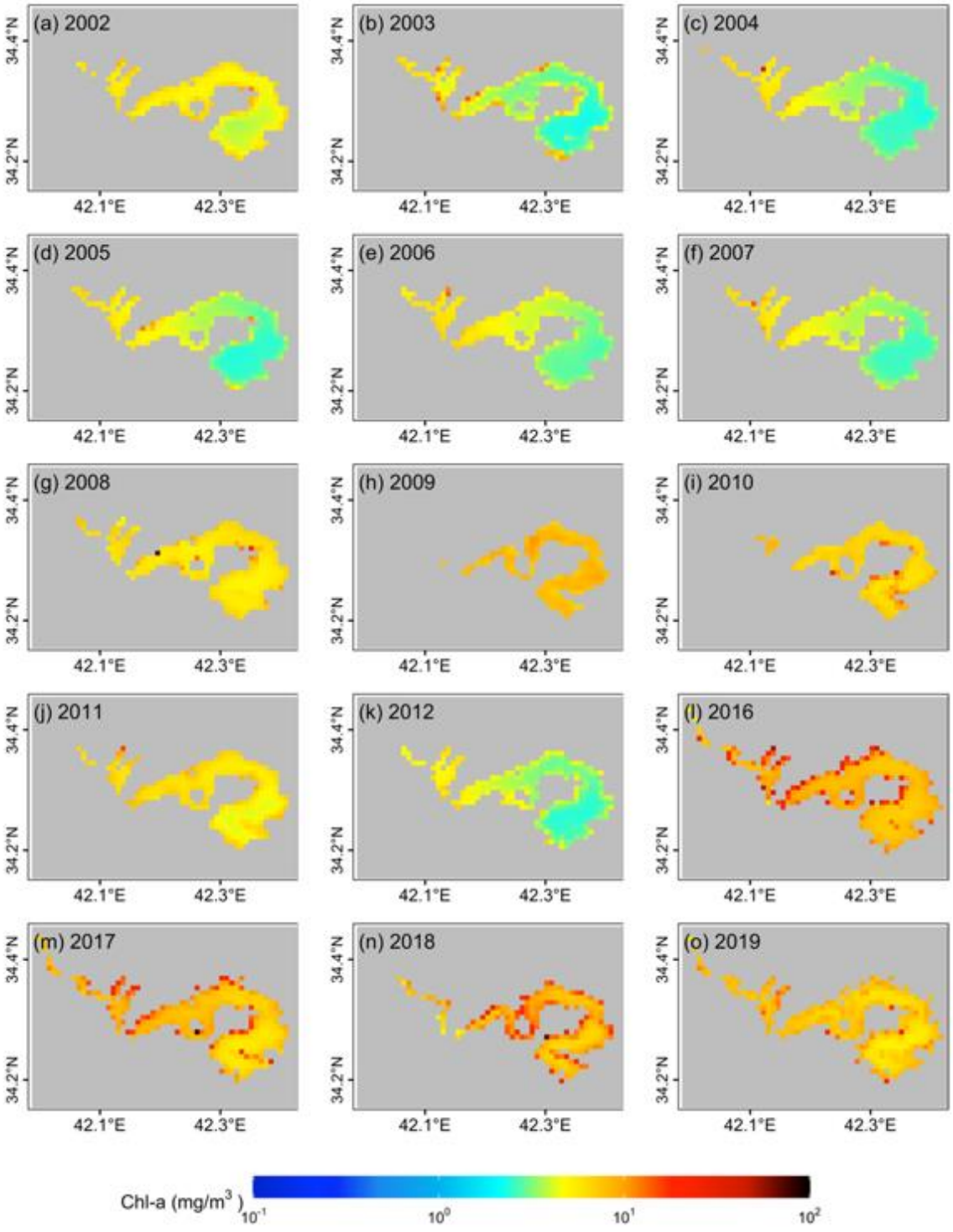

Figure 27. Yearly average Chl-a concentration in Lake Qadisiyah.

Similar to Chl-a concentration, turbidity in the river inflow regions (west part of the lake) was higher than in the east part of the lake (Figure 28). Turbidity was highest in 2008 when the water area was smallest, followed by 2018 when turbidity was higher and water area smaller than most other years.

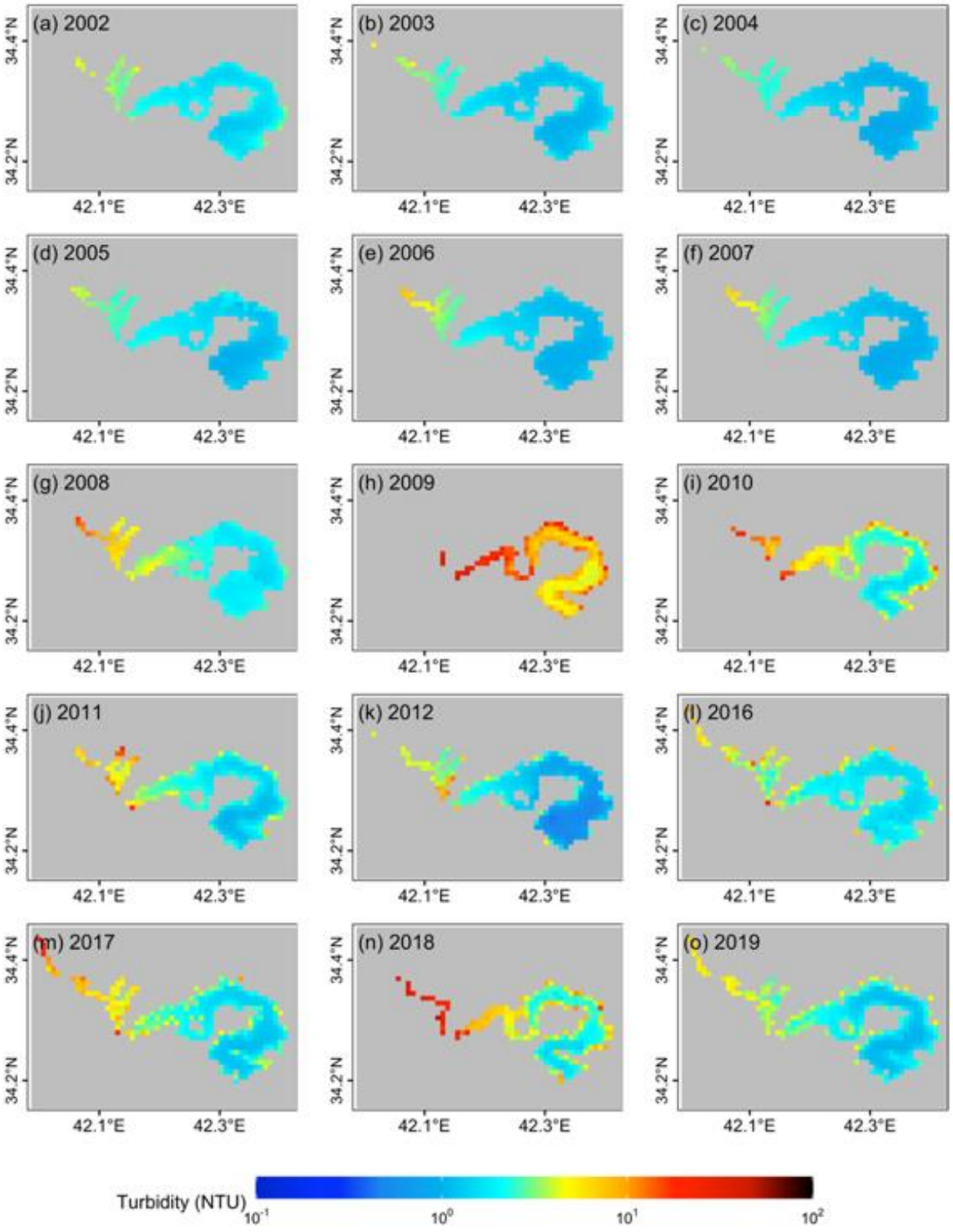

Figure 28. Yearly average turbidity in Lake Qadisiyah.

By analysing the El Niño/Southern Oscillation (MEI), drought (SPI), precipitation, wind speed, air temperature in the lake catchment, we found that MEI and SPI were correlated and show negative relationships with water level in Lake Qadisiyah (Figure 29). Precipitation in the lake catchment during 2007 - 2009 and 2017 - 2018 was clearly lower than other years. In addition, water level decrease happened generally 6 months following droughts (Figure 29 panels b versus c).

Therefore, we conclude a probably link between water level decrease in 2001 - 2002, 2007 - 2011, and 2017 - 2019 with El Niño events, which led to lower precipitation in the lake catchment and drought. Reduced water inflow from catchment to the lake amid water use, evaporation and outflow from the lake led to a reduced water level. Decrease of water level finally led to Chl-a concentration and turbidity increase, with possible reasons of higher nutrient load (or lower dilution), atmospheric deposition from the catchment during drought, and stronger sediment resuspension because of the reduced water level.

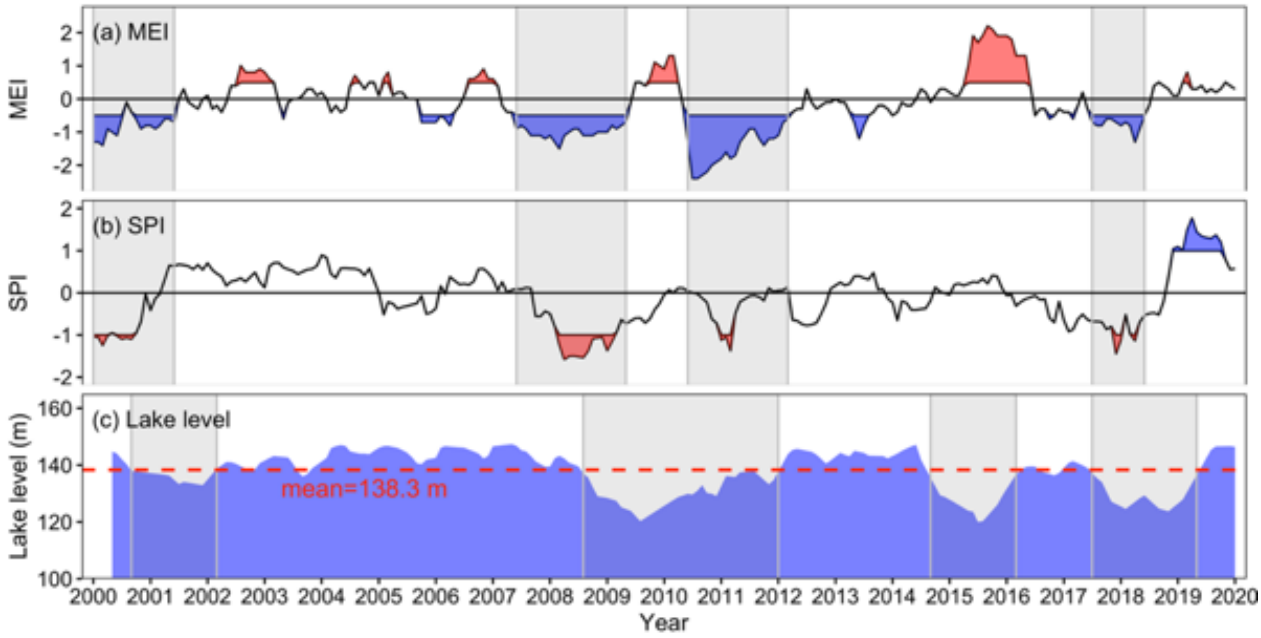

Figure 29. (a) El Niño/Southern Oscillation (ENSO) index (MEI), (b) standardised precipitation index (SPI) in Lake Qadisiyah catchment, and (c) water level during 2000-2019. Red and blue areas in (a) indicate MEI higher than 0.5 and lower than -0.5 respectively. Red and blue areas in (b) indicate SPI higher than 1 and lower than -1 respectively.

8.3 Aggregated climate indicators for the global lakes dataset (BC)

Indicators that help to assess climate impacts on lakes were generated based on the Lakes_cci dataset. The initial effort for the climate impact indicator set came from the German Adaptation Strategy (*Deutsche Anpassungsstrategie*, DAS). This strategy addresses the impacts of climate change in Germany and is designed to help the country adapt and minimize associated risks and vulnerabilities. The strategy was developed by the German Federal Government in response to the growing awareness of climate change and its potential consequences. 120 indicators are defined to monitor and evaluate the state of adaptation and climate change impacts in various sectors, including water quality and management indicators supported by satellite observation. While a national strategy is crucial for understanding and addressing climate change impacts, a global dataset enables other countries to develop those strategies. Here, we focus on the development of lake climate change indicators at the global scale.

In addition to the indicator set, which provide a comprehensive view of trends and vulnerabilities in lakes, a user-friendly visualisation dashboard was developed to make the resulting indicators accessible and understandable to a diverse audience, including policymakers, researchers, and the public. This approach ensures that the insights drawn from the data can be effectively communicated and utilized for informed decision-making and climate adaptation efforts.

8.3.1 Lakes_cci climate indicators

The initial set of indicators consists of three metrics. It is our objective to expand this set in the future. The initial indicators were selected because of their high data quality, direct relevance to climate change and relatively high data density.

8.3.1.1 Temperature anomaly

The first indicator is the temperature anomaly in lakes. This indicator is crucial for understanding variations in lake temperatures, providing valuable insights into the impact of climate change on aquatic ecosystems. By analysing temperature anomalies in lakes, we can assess the thermal health of these ecosystems, which is vital for biodiversity, water quality, and overall environmental resilience. The indicator is calculated on the LSWT data of quality levels 4 and 5 to ensure data reliability. To calculate this indicator, a deseasonalised lake median time series is created. This process removes the influence of seasonal variation, isolating long-term temperature trends. Additionally, the analysis focuses on the five warmest months of the year, selected based on the climatology. Only products with at least 20% valid pixels are used. The final indicator provides a yearly mean of the water temperature anomaly (see example Figure 30).

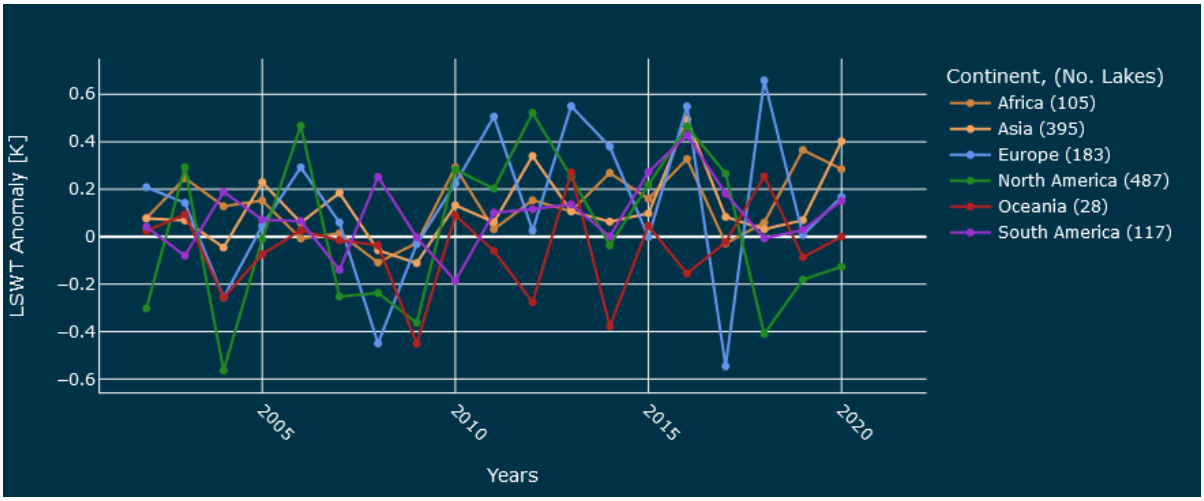

Figure 30. Time series of the lake surface water temperature (LSWT) anomaly aggregated by continent.

8.3.1.2 Heatwaves

The second indicator assesses extreme temperature events in lakes (Figure 31). It follows a methodology similar to the first indicator using LSWT data with quality levels 4 and 5, specifically focusing on the five warmest months of the year and using only daily products with at least 20% valid pixels. A heatwave, is defined here as the lake median temperature exceeding the seasonal 90th percentile of the full time series from 2002-2020, lasting at least two consecutive days within a 5-day period. This methodology follows Hobday et al. (2016) and Woolway et al. (2021). The final metric is determined by counting, per lake, the number of days classified as heat waves, during a given year. This indicator helps us gauge the frequency and intensity of extreme temperature events in lakes, which can have significant ecological and environmental implications.

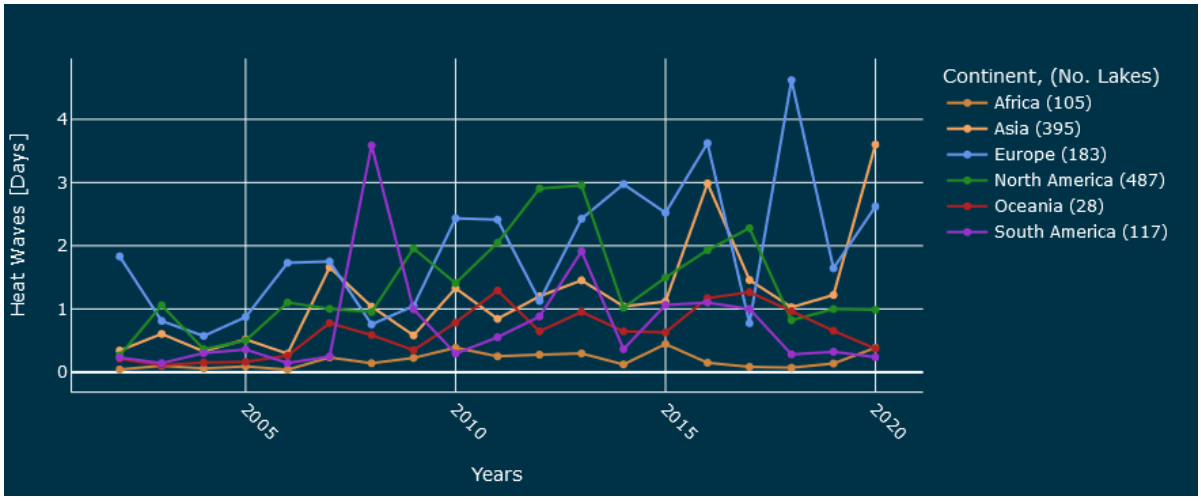

Figure 31. Time series of heatwave-days for the global lakes LSWT data set aggregated by continent.

8.3.1.3 Ice cover

The third indicator is a measure of ice cover in lakes and is calculated by determining the fraction of ice covered pixels in relation to all valid pixels (Figure 32). This means that it quantifies the proportion of the water surface covered by ice during a specific period, irrespective of lake size. The indicator provides insights into the extent and stability of ice in the region of interest. This indicator is valuable for assessing the impact of a changing climate on the presence of ice in lakes, which is significant for various ecological and hydrological processes.

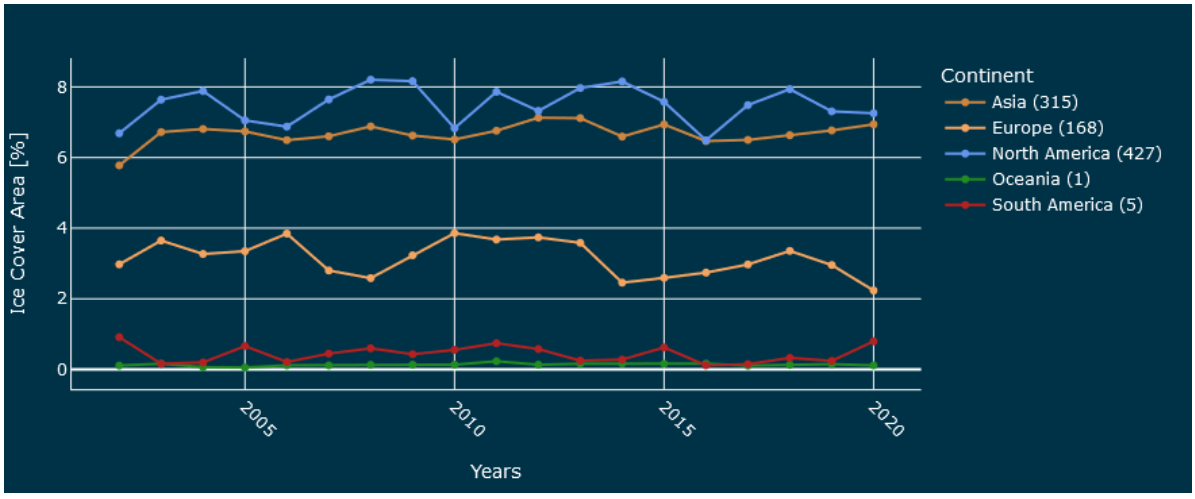

Figure 32. Time series of the global lakes ice coverage area aggregated by continent.

By assessing indicators at the lake level, we gain insights into how individual water bodies respond to climate change, which is critical for understanding ecological impacts and adaptation needs on a local level. Simultaneously, the aggregation of these lake-level indicators into larger properties provides a broader context for a national or global analysis. This approach enables us to identify broader regional or global trends, differences in climate zones, and the influence of lake characteristics on climate change impacts. By leveraging both views, this methodology enhances the overall applicability of our indicators, supporting more informed decision-making and adaptation strategies that can be tailored to specific regions. Lake properties used for the grouping of lakes are collected from the HydroLakes which provides 56 hydrology, physiography, climate and anthropogenic variables. The following aggregation methods are

available within the dashboard: continent, lake surface area, lake average depth, climate zone, elevation, population density, annual precipitation, water residence time and lake water volume.

8.3.2 Visualisation of climate indicators

A user-friendly browser-based dashboard was developed for easy access to the indicators and their behaviour for different lake groups. The dashboard can be accessed via the following link:

https://lakescci.climate-indicators.brockmann-consult.de/

This dashboard provides an interactive and comprehensive platform for users to explore and understand the indicator results (Figure 33). It features a global map showcasing the spatial distribution of the lakes and incorporates a range of critical information, including time series data, trend analyses, and indicator distributions. Users can select specific indicators and even narrow down their focus to individual countries, making it a versatile tool for anyone interested in tracking indicator development, whether at a global or national level. Additionally, single lakes can be selected in the dashboard and compared to the indicator values of the aggregated levels. This flexibility, coupled with its interactive features, empowers users to gain valuable insights into the impact of climate change and aids in informed decision-making for environmental and climate adaptation efforts.

Figure 33. Overview of browser-based climate indicator dashboard with interactive selection of the indicator, the aggregation method and a country.

The dashboard not only serves as an analytical tool but is also suitable for raising awareness and promoting the data set to new users. It demonstrates how the data set can be used to understand and address climate change impacts. In addition to its scientific applications, the dashboard is designed to be accessible to non-scientific experts. It offers a user-friendly platform that provides quick overviews of the indicators for lakes, making it a valuable resource for decision-makers, policymakers, and local authorities interested in understanding the state of lakes globally or on a national level in the context of climate change. Thus, the indicators and the dashboard are serving both scientific and policy purposes.

8.3.3 Examples

8.3.3.1 Ice Cover in Greenland

In Greenland, the dashboard has proven helpful in witnessing the impact of climate change on lake ice cover. The lake ice cover indicator shows a clear and concerning trend. It points to a significant decrease in lake ice cover, with lakes at altitudes < 1000m showing a decline in ice cover by -20% every 10 years, while a decline is visible also at lower elevations. The geographical location of the lakes, whether they are situated in the northern or southern parts of Greenland, does not seem to be influential in this phenomenon (Figure 34).

The years 2016 and 2019 stand out with low ice cover, whereas a peak was observed in 2009. The lake ice cover indicator demonstrates substantial ice loss during these years. This can be compared to the melt extent of the Greenland ice sheet in 2019, showing an increased melting during this year Temperatures in certain areas of Greenland surged by 10°C above the average in 2019, and at the summit of the ice sheet, which sits over 3,200 meters above sea level, temperatures intermittently exceeded the freezing point for extended periods. Additionally, the months of April, May, June, and July witnessed temperatures consistently surpassing the typical averages across Greenland (Duncombe 2019). While direct comparison between lake ice cover loss and the melting of Greenland ice is not feasible, the findings reveal parallel trends. These observations suggest the potential for utilizing the showcased indicator to pinpoint notable years of fluctuation in lake ice cover areas.

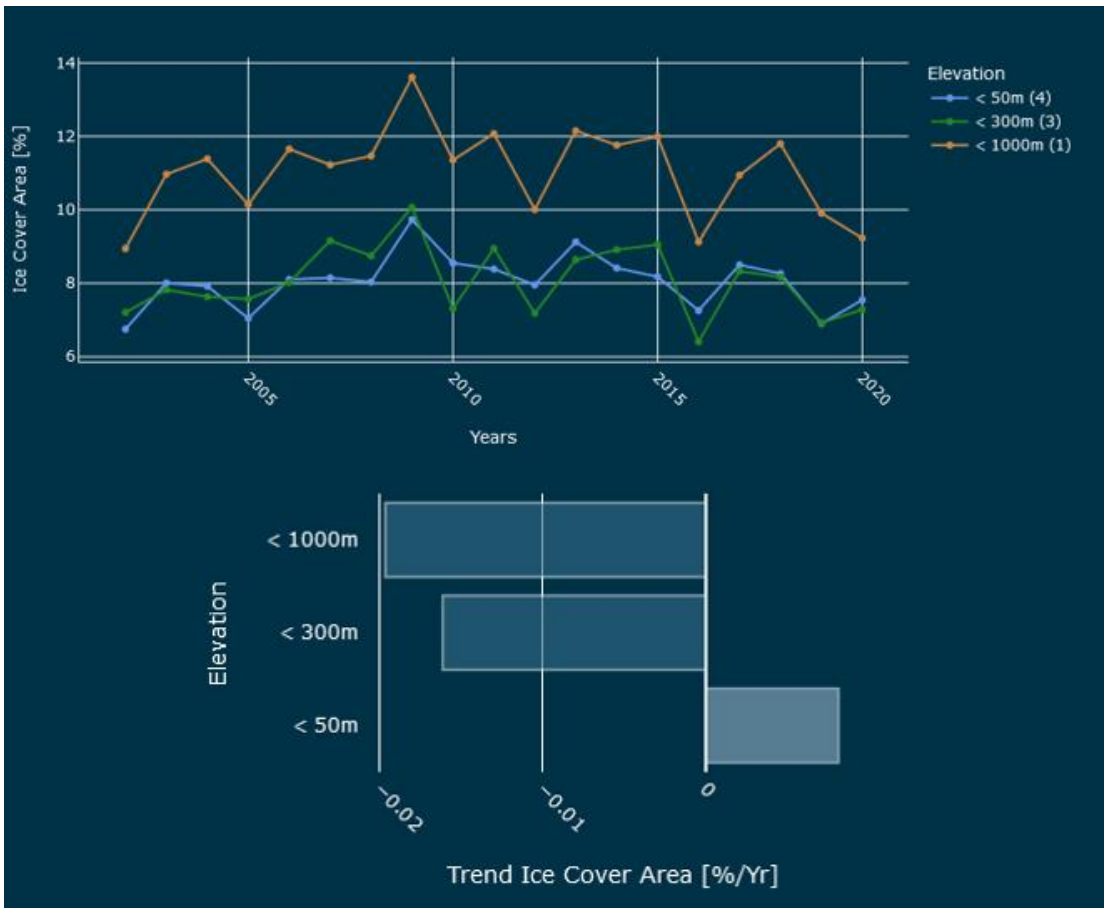

Figure 34. Time series of ice cover area in Greenland aggregated by lake elevation.

8.3.3.2 Heatwaves in Sweden

The dashboard for heatwaves indicates a concerning trend in Sweden. It reveals a notable increase in the frequency and intensity of heat waves in Swedish lakes over recent years. Heatwaves are impacting lakes throughout the country.

The data, especially for smaller lakes, highlights the vulnerability of these water bodies to rising temperatures. Lakes with a water surface area < 300 km² are affected by increasing number of heatwaves at a rate of one additional heatwave-day every 10 years. One standout example is the year 2018, which was exceptionally warm. The heatwave indicator illustrates this by showcasing a significant spike in the number of heatwave-days in lakes across Sweden during that year (Figure 35). Wilcke et al. 2020 demonstrated that the summer 2018 notably deviates from the typical climate patterns observed. May's average temperature appears particularly exceptional compared to historical observations. Furthermore, average temperatures for July and the four-month span from May to August significantly exceed previous maximums recorded in southern Sweden. This illustrates the functionality of the dashboard to capture trends as well as specific anomalous periods.

Figure 35. Time series of heat wave counts in Sweden aggregated by the water surface area.

9 Progress on user requirements

9.1 Updates on user requirements

Differences in user needs between applications emerged from the analysis of the various sources of user requirements. The GCOS observation requirements (GCOS 2022), which sets Threshold (T), Breakthrough (B) and Goal (G) levels is summarized in Table 2. It is important to recall that this is a synthesis of what is required and not a statement of what will or can be achieved using satellite observation.

Table 2. Summary of target GCOS requirements for the Lakes ECV ("2-sigma"). Thematic ECVs are Lake Water Level (LWL), Lake Water Extent (LWE), Lake Surface Water Temperature (LSWT), Lake Ice Cover (LIC), Lake Ice Thickness (LIT), Lake Water Leaving Reflectance (LWLR).

		Requirements											
		LWL		**LWE**		**LSWT**		**LIC**		**LIT**		**LWLR**	
Item needed	*[1]*	Value	Unit	Value	Unit	Value	Unit	Value	Unit	Value	Unit	Value	Unit
Horizontal Resolution	G	-		10		0.1		50		50		10	
	B	-	m	30	m	1	km	100	m	1000	m	100	m
	T	100		1000		2		1000		10000		1000	
Temporal Resolution	G	1		5		3		<1		1		<1	
	B	30	d	-	d	24	h	1	d	30	d	1	d
	T	365		30		240		3-7		365		3-30	
Timeliness	G	1		5		1		1		1		1	
	B	30	d	-	d	30	d	-	d	30	d	30	d
	T	365		365		365		365		365		365	
Required Measurement Uncertainty (2-sigma)	G	5		5		0.1		1		1		10*[2]*	
	B	-	cm	-	%	0.3	°C	-	%	10	cm	20	%
	T	10		-		0.6		10		15		30	
Stability	G	1		5		0.1		0.1		1		0.1	
	B	-	cm/decade	-	%/decade	-	°C/decade	-	%	-	cm	0.5	%/decade
	T	10		-		0.25		1		10		1	

[1] Goal (G): an ideal requirement above which further improvements are not necessary. Breakthrough (B): an intermediate level between threshold and goal which, if achieved, would result in a significant improvement for the targeted application. The breakthrough value may also indicate the level at which specified uses within climate monitoring become possible. It may be appropriate to have different breakthrough values for different uses. Threshold (T): the minimum requirement to be met to ensure that data are useful.

[2] Equivalent to 10-30% for peak waveband vs low signal bands; 0.1 mg m^{-3} chlorophyll-a and 1 g m^{-3} suspended matter or 1 NTU

Here, we report an update of the currently achieved GCOS requirements and an analysis of the remaining gaps for the six Lakes ECVs (Table 3,Table 4, Table 5, Table 6, Table 7, Table 8).

Table 3. Summary of threshold and target of GCOS requirements for the lake water level (LWL) variable, current status about the achievement of the requirements.

Property	Threshold	Target/Goal	Currently Achieved	Gap analysis
Spatial coverage	Global	Global	> 500 lakes	Increase coverage (ongoing activity).
Temporal coverage	10 years	>25years	More than 30 years for some lakes	Target reached
Spatial resolution	Area: 1000 km²	Area: 1 km²	Lakes > 30 km²	Threshold reached. New algorithms must be implemented to improve resolution. New missions / altimeters needed to reach target (e.g. SWOT).
Temporal resolution	1 - 10 days	Daily	1 - 10 days	Threshold reached. New missions / altimeters needed to reach target.
Standard uncertainty of LWL	15 cm	3 cm for large lakes, 10 cm for the remainder.	10cm for large lakes, 20 cm for medium lakes, small lakes not processed.	Threshold reached for most lakes in the product. New algorithms must be developed to reach target. New missions / altimeters will help to reach the target (e.g. SWOT).
Trend uncertainty (stability)	-	1 cm / decade	Not estimated. For comparison, on oceanic surfaces, the trend uncertainty has been estimated up to 5 cm / decade locally.	-

Table 4. Summary of threshold and target of GCOS requirements for the lake surface water temperature (LSWT) variable, current status about the achievement of the requirements.

Property	Threshold	Target/Goal	Currently Achieved	Gap analysis
Spatial coverage	Global	Global	> 2000 lakes	Use of a higher resolution sensor such as VIIRS is needed to increase the success rate for smaller lakes.
Temporal coverage	10 years	>25years	> 25 years	Target reached
Spatial resolution	0.1°	10 – 5000 m	~0.008° (gridded)	
Temporal resolution	Weekly	Between 3 hours and 10 days	Variable because of clouds and variable spatial resolution across satellite swaths. Daily for large lakes under clear skies.	Effective temporal resolution increases as further MetOp/SLSTR/MODIS input data streams are exploited.
Standard uncertainty of LSWT	1.0 K	Between 0.1 K and 0.6 K	Standard deviation of single-pixel differences to *in situ* are typically ~0.5 K (for best quality levels).	Addition of MetOp-C input data streams reduces uncertainty from averaging of LSWTs over multiple observations.

Trend uncertainty (stability)	Between 0.01 and 0.025 K yr^{-1}	Between 0.01 and 0.025 K yr^{-1}	Difficult to assess as there are no reference networks of known stability.	Need to continue to collect as much *in situ* data as possible, including retrospectively.

Table 5. Summary of threshold and target of GCOS requirements for the lake water extent (LWE) variable, current status about the achievement of the requirements.

Property	Threshold	Target/Goal	Currently Achieved	Gap analysis
Spatial coverage	Global	Global	>200 lakes	
Temporal coverage	10 years	>25years	More than 30 years for some lakes	Will depend on the length of the altimetric coverage
Spatial resolution	10 m	1000 m	10-30 m	Target reached
Temporal resolution	5 days	30 days	1-10 days	After obtaining the hypsometric relationship between LWL and LWE, the temporal resolution will be finally based on the altimetric satellite revisit
Standard uncertainty of LWE	5%	3%	Between 1 and 10%	Post processing under development to increase the accuracy
Trend uncertainty (stability)	2.5%		Not assessed.	To be quantified.

Table 6. Summary of threshold and target of GCOS requirements for the lake ice cover (LIC) variable, current status about the achievement of the requirements.

Property	Threshold	Target/Goal	Currently Achieved	Gap analysis
Spatial coverage	Global (where ice forms)	Global (where ice forms)	> 1300 lakes	Increased coverage is possible but currently outside the scope of Lakes_cci.
Temporal coverage	10 years	>25 years	> 20 years	Threshold reached.
Spatial resolution	1000 m	50 m	250 m	Threshold reached. Target possible from Landsat/Sentinel-2 analysis to the detriment of temporal resolution (not meeting threshold).
Temporal resolution	3-7 days	<1 day	Daily for lakes under clear sky conditions.	Threshold reached under clear sky conditions from multiple satellite acquisitions. Development of gap- filling approach is needed to reach target when cloud cover persists for several days/weeks.
Standard uncertainty of LIC	10%	1%	Overall classification accuracy is 0.83% for open water, 3.07% for cloud cover, and 2.23% for ice cover . The same accuracy value is assigned to each pixel of the same class.	Pixel-based uncertainty quantification is ongoing. Assessment of the threshold (10%) of ice cover extent is ongoing.
Trend uncertainty (stability)	1%	0.1%	Not assessed.	To be quantified.

Table 7. Summary of threshold and target of GCOS requirements for the lake ice thickness (LIT) variable, current status about the achievement of the requirements.

Property	Threshold	Target/Goal	Currently Achieved	Gap analysis
Spatial coverage	Global (where ice forms)	Global (where ice forms)	Great Slave Lake	Increased coverage (ongoing activity).
Temporal coverage	10 years	>25 years	> 20 years	Threshold reached.
Spatial resolution	1000 m	50 m	10000 m	Threshold reached.
Temporal resolution	365 days	Daily	10 days	Threshold reached.
Standard uncertainty of LIT	15 cm	1 cm	10 cm	Threshold reached.
Trend uncertainty (stability)	10 cm	1 cm	Not assessed.	To be quantified.

Table 8. Summary of threshold and target of GCOS requirements for the lake water leaving reflectance- (LWLR) variable, current status about the achievement of the requirements.

Property	Threshold	Target/Goal	Currently Achieved	Gap analysis
Spatial coverage	Global	Global	> 2000 lakes	> 4000 lakes observable, cf. Copernicus Land Monitoring Service
Temporal coverage	10 years	>25years	> 20 years with a 4-year gap	Further effort needed to gap-fill, assess stability, with MODIS
Spatial resolution	10 m	1000 m	300 - 1000 m	Higher resolution not possible for full time-series (2012-2016). 10-60m resolution feasible using land sensors (limited sensitivity)
Temporal resolution	<1	3-30 days	Up to daily	Target reached. Daily observation (not accounting for cloud) possible from ~2017 onward.
Standard uncertainty of LWLR	10%	30%	In terms of Chl-a, 90% of reported pixel uncertainty ranged 39-60%. In terms of Turbidity, 90% of reported pixel uncertainty ranged 59-80%	Threshold not reached, also owing to large uncertainty in models to express uncertainty, which are limited by scarce in situ observation data.
Trend uncertainty (stability)	0.1 % per decade	1 % per decade	Not assessed.	To be quantified.

In addition to the needs of the climate community, a wider community of users interested in lake investigations are specialists in limnology, hydrology, ecology and biogeochemistry. The main applications are in ecological modelling, exploring the effects of environmental changes and assessing temporal and spatial trends. This wider community, responding to the last survey reported in URD v1, highlighted a number of recommended improvements to the Lakes_cci dataset.

The recommended improvements included the increase of the number of lakes, which has already been partially improved with dataset v2.0.2, with an expansion to 2024 regions that is met by LWLR, LWST and LIC (for ice-forming lakes). Expansion of the dataset covered by LWE (extension of hypsometry calculation using the Sentinel-2 mission) and LWL (new software for small lakes and new data product for historical missions) continues into CRDP v2.1 and beyond. Other requested improvements were to increase data frequency and data quality, and to provided gap-filled time series. Data quality control, through flags, uncertainty characterisation, and masking have also been improved towards version 2.1 of the dataset, which will be available to users in early 2024. Users further suggested adding coloured dissolved organic

matter (CDOM) and vertical diffuse attenuation (K_d) through survey responses. Activities to select and implement CDOM algorithms are underway.

Further updates per ECV product expected to be released in v2.1.0 are as follows:

- LWL: increase in spatial coverage; improvement in time series due to geoid correction (after 2020); increase in spatial and temporal coverage using data from previous satellite missions.
- LWE: increase in spatial coverage, and validation of the LWE extraction process from Sentinel-2.
- The LSWT ECV showed an update in temporal scale with the processing of MODIS/Terra and the reprocessing of SLSTR/Sentinel-3A/B for v2.1.
- LIC: the main improvement concerned the classification accuracy of the Random Forest (RF) algorithm and the estimation of uncertainty from the overall to the per-pixel level, in order to ensure a more accurate product. In addition, validation, and inter-comparison of LIC, together with the derived ice phenology with other lake ice products, were performed.
- LWLR: for LWLR and Chl-a, 48 lakes (8 added) can be provided with MODIS-Aqua during 2012-2016, to fill the existing gap. Updated quality flags include a new quality flag from climatological filtering (consistency) in addition to flags related to the pixel identification and atmospheric correction. These updates and improvements may enhance the handling of the dataset for users.

A technical note on "CDOM algorithm assessment for a global distribution of lakes" was produced in parallel to the work presented here. This includes information on in situ data collection, algorithm comparison and testing, assessment, and selection of published CDOM algorithms, as well as recommendations for waterbodies types. In addition, it includes a list of optical water types for which the existing CDOM algorithms can obtain CDOM and areas in which further research is required to raise the accuracy of CDOM estimations.

From the last "13th CCI Colocation & CMUG Integration meetings" held in Oxford between 7th and 9th November 2023, the following summary focus on item useful for user requirement analysis.

- The GCOS Revised Implementation Plan (2022) specifically recommended that more emphasis should be placed on merging individual ECVs, in order to address unresolved challenges in the energy, water and carbon cycles.
- GCOS plans to host one or more workshops with leading adaption implementers and experts, in order to discover global datasets, ECVs, and climate data, with spatial and temporal requirements for adaptation. When questioned about the amount of satellite data needed for adaptation, GCOS recommended using high-resolution space-based observations (≃10m) to design adaption actions and to monitor changes at the local scale. Expanding on ESA adaptation strategies, a summary was given of the many applications of satellite data for health adaptation, highlighting the expertise and accessibility of these data. Despite the drawbacks of using space data for adaptation, successful adaptation depends on policy makers having a better understanding of the data and access to ready-to-use data. In addition, the spatial and temporal resolution of the data is crucial for local applications.
- The CMUG Integration session began with an overview of the new 3-year phase of CMUG, focusing on the consortium partners and on the main work packages of the project. This was followed by a summary of the planned CMUG scientific studies using CCI ECV data in the context of climate models.

The user requirements will be further updated with the next URD v2 (Apr 2024).

A user workshop will be organised in spring-summer 2024, possibly together with the Physical Processes in Natural Waters Workshop (PPNW) 2024, with the aim of presenting the ECV products to the wider user community outside the CCI and to collect and discuss user feedback. The workshop should be attended by use case studies partners who will also present their case study experiences. The workshop will also

invite CMUG as well as other stakeholders involved in the Lakes_cci since its inception. The outcome of the workshop will be also included in CAR v2.

10 External studies

A preliminary overview of external scientific studies based on the Lakes_cci dataset is presented in this final section.

To improve lake temperature modelling and to investigate the complexities of surface water temperature trends and heatwaves occurrence in Chinese lakes from 1980 to 2100, Wang et al. (2023) combined satellite measurements with a numerical model. Climate forcing from ERA5-Land were used to drive the FLake model during historic period, and the model has been fine-tuned using the Lakes_cci LSWT data, resulting in a projection of future change.

In another recent paper on "Temporal changes in the remote sensing reflectance at Lake Vänern" by Cazzaniga et al. (2023), satellite-derived LSWT, Chl-a and turbidity products from the Lakes_cci dataset were considered in addition to MODIS-A data. After evaluating their accuracy against in situ data, which gave good fit results, it was possible to use these products in the subsequent study. Specifically, only pixels marked as "best quality data" were included in the average of 3 x 3 pixels (i.e. ~ 9 km^2) centered on the in situ stations.

The Lakes_cci LSWT dataset was taken into consideration in the study of Calamita et al. (2023) on the identification of lake mixing anomalies. Long-term lake warming is frequently illustrated in terms of spatial averages using remotely detected lake surface water temperatures. The objective of this study was to evaluate the long-term variability in the mixing of large lakes in the context of climate change. To that end, the horizontal data gradients were utilized to better understand internal dynamics of lakes and to identify lake mixing anomalies. The authors employed a method known as ‘thermal front tracking’, which is far more common in oceanography than in limnology, to find mixing anomalies in dimictic lakes throughout the globe.

In the paper by Zhao et al. (2023), entitled "Dynamic monitoring and analysis of chlorophyll-a concentrations in global lakes using Sentinel-2 images in Google Earth Engine", mean Chl-a concentration was estimated for 3067 globally distributed lakes for the period 2019-2021 by applying different algorithms to Sentinel-2 images based on Optical Water Type classification using GEE. Lakes_cci Chl-a data were used as auxiliary data and Chl-a monthly average was chosen to validate the retrieved Chl-a in this study.

11 Conclusions

This report describes a first exploration of the Lakes_cci CRDP v2.0.2 and provides an updated global overview of the data distribution with respect to v1.1 of the dataset, providing distribution plots indicating the range of variation for the set of variables considered. The code to extract ECV data followed recommendations (e.g. uncertainties, quality flags) from the PUG and PSD documents, with additional post-processing operations such as gap filling when necessary.

Analyses and assessments carried out in the studies presented in the report include different applications of the Lakes_cci dataset, ranging from local to regional and global scales. In the case of Lake Garda (Italy), LSWT time series were combined with modelling to estimate lake evaporation. LSWT, Chl-a and turbidity were used to obtain the dominant modes explaining spatio-temporal variability of these variables in lake water.

At the regional scale, a subset of South American lakes covering a range of geographical sub-regions, lake morphological characteristics and trophic status, was selected and a preliminary trend analysis of the Lakes_cci variables LSWT, Chl-a and turbidity was carried out, together with meteo-climatic variables. In addition, a first application of the climate indicators 'LSWT anomaly' and 'heatwaves', developed within the Lakes_cci project, was carried out revealing geographical patterns.

At the global scale, a specific analysis focused on shallow lakes, which are particularly vulnerable and sensitive to the effects of climate change. A preliminary trend analysis of LSWT, Chl-a and turbidity data for 352 shallow lakes was presented, emphasizing the potential of the CCI dataset in providing a global picture of changes in lake water quality variables. Another study utilized LSWT data of the upcoming 2024 Lakes_cci release, subdivided for climatic regions, to test the potential performance of a neural network machine learning approach in simulating and predicting LSWT dynamics and in identifying the most significant climate variables.

This CAR further provides an overview of the preliminary results of three specific use cases. Lakes_cci variables were used to understand the response of lakes to the European 2019 heatwave showing continental-scale and lake morphological responses. LWL, Chl-a and turbidity were combined to study long-term change in a reservoir (Lake Qadisiyah, Iraq) located in a hot desert climate to investigate the influence of La Niña on water quantity and quality. Finally, new functionality for the Climate Indicators Dashboard and the potential of using these climate indicators were demonstrated in various regions.

We remind the reader that this report represents a first assessment of v2 of the dataset. Final results and conclusions from several ongoing studies will be presented in 2025 with the next version of this report. The Climate Research Group will carry out many of these activities in the coming months, including further use case development and the preparation of scientific publications.

A summary and update of user requirements was reported in this document. In particular, current progress towards the GCOS requirements 2022 was assessed. An update on the current status compared to threshold, breakthrough and goal targets is reported, highlighting remaining gaps.

Finally, a section of the report provides an initial review of the results of external studies that examined and tested the Lakes_cci data set, showing increasing interest in these data independent of our own work. We believe that this is partly due to the successful dissemination activities of the Lakes_cci team. These efforts will continue in the near future by attending conferences, preparing manuscripts and promoting the dataset in various communities.

12 References

Amadori, M., Bresciani, M., Giardino, C., Dijkstra, H. Lakes surface mixed layers slowly integrate fast atmospheric variability: Evidence from a deep perialpline lake, under review.

Amadori, M., Giovannini, L., Toffolon, M., Piccolroaz, S., Zardi, D., Bresciani, M., Giardino, C., Luciani, G., Kliphuis, M., van Haren, H., and Dijkstra, H. A. (2021). Multi-scale evaluation of a 3D lake model forced by an atmospheric model against standard monitoring data. Environmental Modelling & Software, 139:105017

Blanken, P. D., Spence, C., Hedstrom, N., & Lenters, J. D. (2011). Evaporation from Lake Superior: 1. Physical controls and processes. Journal of Great Lakes Research, 37(4), 707-716.

Bresciani, M., Giardino, C., Boschetti, L. (2011). Multi-temporal assessment of bio-physical parameters in lakes Garda and Trasimeno from MODIS and MERIS. European Journal of Remote Sensing, 43:49–62.

Calamita, E., Brechbühler, M., Woolway, I., Albergel, C., and Odermatt, D. (2023). Detecting lake mixing anomalies using Earth Observation, EGU General Assembly, Vienna, Austria, 24–28 Apr 2023, EGU23-15065, https://doi.org/10.5194/egusphere-egu23-15065, 2023.

Carrea, L., Crétaux, J. F., Liu, X., Wu, Y., Calmettes, B., Duguay, C. R., ... & Albergel, C. (2023a). Satellite-derived multivariate world-wide lake physical variable timeseries for climate studies. Scientific Data, 10(1), 30.

Carrea, L., Merchant, C.J, Cretaux, J.-F., Dokulil, T. M., Dugan, H. A., Gibbes, B., Laas, A., Leibensperger, E. M., Maberly, S., May, L., Matsuzaki, S.-I., Monet, G., Pierson, D., Pulkkanen, M., Rusanovskaya, O. O., Shimaraeva, S. V., Silow, E. A., Schmid, M., Timofeyev, M. A., Verburg, P., Woolway, R. I. (2023b). Lake surface water temperature. [in "State of the Climate in 2022"] Bulletin of the American Meteorological Society, 104 (9). S28-S30. ISSN 1520-0477 doi: https://doi.org/10.1175/2023BAMSStateoftheClimate.1

Carslaw, D. C., Ropkins K. (2012). «openair — An R package for air quality data analysis». Environmental Modelling & Software 27–28 (gennaio): 52–61. https://doi.org/10.1016/j.envsoft.2011.09.008.

Castellanos, E., M.F. Lemos, L. Astigarraga, N. Chacón, N. Cuvi, C. Huggel, L. Miranda, M. Moncassim Vale, J.P. Ometto, P.L. Peri, J.C. Postigo, L. Ramajo, L. Roco, M. Rusticucci (2022). Central and South America. In: Climate Change 2022: Impacts, Adaptation and Vulnerability. Contribution of Working Group II to the Sixth Assessment Report of the Intergovernmental Panel on Climate Change [H.-O. Pörtner, D.C. Roberts, M. Tignor, E.S. Poloczanska, K. Mintenbeck, A. Alegría, M. Craig, S. Langsdorf, S. Löschke, V. Möller, A. Okem, B. Rama (eds.)]. Cambridge University Press, Cambridge, UK and New York, NY, USA, pp. 1689–1816, doi:10.1017/9781009325844.014.

Cazzaniga, I., Zibordi, G., Alikas, K., Kratzer, S. (2023). Temporal changes in the remote sensing reflectance at Lake Vänern. Journal of Great Lakes Research, 49(2), 357-367.

Dalton, J. (1802). Experimental Essays on the Constitution of Mixed Gases: On the Force of Steam or Vapour from Water or Other Liquids in Different Temperatures, Both in a Torricelli Vacuum and in Air; on Evaporation; and on Expansion of Gases by Heat. Memoirs of the Literary and Philosophical Society of Manchester, 5, 536-602.

Deng J., Paerl H.W., Qin B., Zhang Y., Zhu G., Jeppesen E., Cai Y., Xu H., (2018). Climatically-modulated decline in wind speed may strongly affect eutrophication in shallow lakes. Science of Total Environment 645, 1361–1370.

Duncombe, J. (2019), Greenland ice sheet beats all-time 1-day melt record, *Eos, 100*, https://doi.org/10.1029/2019EO130349. Published on 02 August 2019.

Feuchtmayr H., Moran R., Hatton K., Connor L., Heyes T., Moss B. Harvey I. and Atkinson D. (2009). Global warming and eutrophication: effects on water chemistry and autotrophic communities in experimental hypertrophic shallow lake mesocosm Journal of Applied Ecology 2009, 46, 713–723

Fichot, C. G., Matsumoto, K., Holt, B., Gierach, M. M., & Tokos, K. S. (2019). Assessing change in the overturning behavior of the Laurentian Great Lakes using remotely sensed lake surface water temperatures. Remote Sensing of Environment, 235, 111427.

Fink, G., Schmid, M., Wahl, B., Wolf, T., & Wüest, A. (2014). Heat flux modifications related to climate-induced warming of large European lakes. Water Resources Research, 50(3), 2072-2085.

Frankignoul, C., & Hasselmann, K. (1977). Stochastic climate models, Part II Application to sea-surface temperature anomalies and thermocline variability. Tellus, 29(4), 289-305.

Free, G., Bresciani,M., Pinardi,M., Simis,S., Liu,X., Albergel, C., Giardino,C. (2022). Investigating lake chlorophyll-a responses to the 2019 European double heatwave using satellite remote sensing, Ecological Indicators, 142, 109217, https://doi.org/10.1016/j.ecolind.2022.109217.

Guo, Y., Zhang, Y., Ma, N., Xu, J., & Zhang, T. (2019). Long-term changes in evaporation over Siling Co Lake on the Tibetan Plateau and its impact on recent rapid lake expansion. Atmospheric research, 216, 141-150.

Hari, M., & Tyagi, B. (2021). Investigating Indian summer heatwaves for 2017–2019 using reanalysis datasets. Acta Geophysica, 69(4), 1447-1464.

Hasselmann, K. (1976), Stochastic climate models Part I. Theory. Tellus, 28: 473-485.

Heddam, S., Ptak, M., & Zhu, S. (2020). Modelling of daily lake surface water temperature from air temperature: Extremely randomized trees (ERT) versus Air2Water, MARS, M5Tree, RF and MLPNN. Journal of Hydrology, 588, 125130.

Hobday, A. J., Alexander, L. V., Perkins, S. E., Smale, D. A., Straub, S. C., Oliver, E. C., ... & Wernberg, T. (2016). A hierarchical approach to defining marine heatwaves. Progress in Oceanography, 141, 227-238.

Köppen, W., 1918. Klassifikation der klimate nach Temperatur, Niederschlag und Yahreslauf.Pet. Mitt., 64, pp.193-203.

Lepori, F., Bartosiewicz, M., Simona, M., and Veronesi, M. (2018). Effects of winter weather and mixing regime on the restoration of a deep perialpine lake (lake Lugano, Switzerland and Italy). Hydrobiologia, 824.

Lizana N., 2023. Assessment of climate change effects on water quality of South American lakes using long-term satellite-derived data. Master's thesis in progress.

Llames, M. E., & Zagarese, H. (2009). Lakes and reservoirs of South America. In Elsevier eBooks (pp. 533–543). https://doi.org/10.1016/b978-012370626-3.00034-x

Maberly, S. C., O'Donnell, R. A., Woolway, R. I., Cutler, M. E., Gong, M., Jones, I. D., ... & Tyler, A. N. (2020). Global lake thermal regions shift under climate change. Nature Communications, 11(1), 1232.

Matta, E., Amadori, M., Free, G., Giardino, C., & Bresciani, M. (2022). A Satellite-Based Tool for Mapping Evaporation in Inland Water Bodies: Formulation, Application, and Operational Aspects. Remote Sensing, 14(11), 2636.

Messager, M. L., Lehner, B., Grill, G., Nedeva, I., & Schmitt, O. (2016). Estimating the volume and age of water stored in global lakes using a geo-statistical approach. Nature communications, 7(1), 13603.

Michelutti, N., Cooke, C. A., Hobbs, W. O., & Smol, J. P. (2015). Climate-driven changes in lakes from the Peruvian Andes. Journal of paleolimnology, 54, 153-160.

Milan, M., Bigler, C., Salmaso, N., Guella, G., and Tolotti, M. (2015). Multiproxy reconstruction of a large and deep subalpine lake's ecological history since the middle ages. Journal of Great Lakes Research, 41(4):982–994.

Moss, B., Stephen, D., Alvarez, C., Becares, E., Bund, W. V. D., Collings, S. E., ... & Wilson, D. (2003). The determination of ecological status in shallow lakes—a tested system (ECOFRAME) for implementation of the European Water Framework Directive. Aquatic Conservation: Marine and Freshwater Ecosystems, 13(6), 507-549.

Pareeth, S., Bresciani, M., Buzzi, F., Leoni, B., Lepori, F., Ludovisi, A., ... & Salmaso, N. (2017). Warming trends of perialpine lakes from homogenised time series of historical satellite and in-situ data. Science of the Total Environment, 578, 417-426.

Peel, M. C., Finlayson, B. L., & McMahon, T. A. (2007). Updated world map of the Köppen-Geiger climate classification. Hydrology and earth system sciences, 11(5), 1633-1644.

Piccolroaz, S., Calamita, E., Majone, B., Gallice, A., Siviglia, A., and Toffolon, M. 2016. Prediction of river water temperature: a comparison between a new family of hybrid models and statistical approaches. Hydrological Processes, 30(21), 3901-3917, https://doi.org/10.1002/hyp.10913.

Piccolroaz, S., Toffolon, M., Majone, B. (2013). A simple lumped model to convert air temperature into surface water temperature in lakes. Hydrology and Earth System Sciences, 17(8), 3323–3338. https://doi.org/10.5194/hess-17-3323-2013

Piccolroaz, S., Woolway, R. I., & Merchant, C. J. (2020). Global reconstruction of twentieth century lake surface water temperature reveals different warming trends depending on the climatic zone. Climatic Change, 160(3), 427-442.

Piotrowski, A.P. & Napiorkowski, J.J., 2018. Performance of the air2stream model that relates air and stream water temperatures depends on the calibration method. Journal of Hydrology, 561, 395-412. https://doi.org/10.1016/j.jhydrol.2018.04.016

Quan, Q., Hao, Z., Xifeng, H., & Jingchun, L. (2022). Research on water temperature prediction based on improved support vector regression. Neural Computing and Applications, 1-10.

Rabatel, A., Francou, B., Soruco, A., Gomez, J., Cáceres, B., Ceballos, J. L., ... & Wagnon, P. (2013). Current state of glaciers in the tropical Andes: a multi-century perspective on glacier evolution and climate change. The Cryosphere, 7(1), 81-102.

Rahaghi, A. I., Lemmin, U., Cimatoribus, A., Bouffard, D., Riffler, M., Wunderle, S., & Barry, D. A. (2018). Improving surface heat flux estimation for a large lake through model optimization and two-point calibration: The case of Lake Geneva. Limnology and oceanography: methods, 16(9), 576-593.

Ranasinghe, R., Ruane, A.C., Vautard, R., et al., 2021. Chapter 12: Climate change information for regional impact and for risk assessment. Climate Change 2021: The Physical Science Basis. Contribution of Working Group I to the Sixth Assessment Report of the Intergovernmental Panel on Climate Change. Cambridge University Press.

Read, J. S., Jia, X., Willard, J., Appling, A. P., Zwart, J. A., Oliver, S. K., ... & Kumar, V. (2019). Process-guided deep learning predictions of lake water temperature. Water Resources Research, 55(11), 9173-9190.

Riveros-Iregui, D. A., Lenters, J. D., Peake, C. S., Ong, J. B., Healey, N. C., & Zlotnik, V. A. (2017). Evaporation from a shallow, saline lake in the Nebraska Sandhills: Energy balance drivers of seasonal and interannual variability. Journal of Hydrology, 553, 172-187.

Schaefli, B. & Gupta, H. V. (2007). Do Nash values have value? Hydrological Processes: An International Journal, 21(15):2075–2080. https://doi.org/10.1002/hyp.6825

Scheffer M. & van Nes E. H. (2007). Shallow lakes theory revisited: various alternative regimes driven by climate, nutrients, depth and lake size. Hydrobiologia, 584:455–466.

Scheffer M., Hosper S.H., Meijer M.L., Moss B., Jeppesen E. (1993). Alternative equilibria in shallow lakes. Trends in Ecology & Evolution, 8, 275–279.

Sener, E., Terzi, O., Sener, S. and Kucukkara, R. (2012). Modeling of water temperature based on GIS and ANN techniques: Case study of Lake Egirdir (Turkey). Ekoloji, 21(83), 44-52. https://doi.org/10.5053/ekoloji.2012.835

Sharma, S., Walker, S.C., Jackson, D.A. (2008). Empirical modelling of lake water-temperature relationships: a comparison of approaches. Freshwater biology, 53(5), 897-911. https://doi.org/10.1111/j.1365-2427.2008.01943.x

Søndergaard M., Jensen J.P., Jeppesen E. (2003). Role of sediment and internal loading of phosphorus in shallow lakes. Hydrobiologia, 506, 135–145

Sousa, P. M., Barriopedro, D., García-Herrera, R., Ordóñez, C., Soares, P. M., & Trigo, R. M. (2020). Distinct influences of large-scale circulation and regional feedbacks in two exceptional 2019 European heatwaves. Communications Earth & Environment, 1(1), 48.

Thibeault, J. M., Seth, A., & García, M. (2010). Changing climate in the Bolivian Altiplano: CMIP3 projections for temperature and precipitation extremes. Journal of Geophysical Research: Atmospheres, 115(D8).

Till, A., Rypel, A. L., Bray, A., & Fey, S. B. (2019). Fish die-offs are concurrent with thermal extremes in north temperate lakes. Nature Climate Change, 9(8), 637-641.

Toffolon, M., Piccolroaz, S., Majone, B., Soja, A. M., Peeters, F., Schmid, M., & Wüest, A. (2014). Prediction of surface temperature in lakes with different morphology using air temperature. Limnology and Oceanography, 59(6), 2185-2202.

Vercauteren, N., Bou-Zeid, E., Huwald, H., Parlange, M. B., & Brutsaert, W. (2009). Estimation of wet surface evaporation from sensible heat flux measurements. Water Resources Research, 45(6).

Vuille, M., Bradley, R. S., Werner, M., & Keimig, F. (2003). 20th century climate change in the tropical Andes: observations and model results. Climate variability and change in high elevation regions: Past, present & future, 75-99.

Vuille, M., Francou, B., Wagnon, P., Juen, I., Kaser, G., Mark, B. G., & Bradley, R. S. (2008). Climate change and tropical Andean glaciers: Past, present and future. Earth-science reviews, 89(3-4), 79-96.

Vystavna, Y., Harjung, A., Monteiro, L. R., Matiatos, I., & Wassenaar, L. I. (2021). Stable isotopes in global lakes integrate catchment and climatic controls on evaporation. Nature Communications, 12(1), 7224.

Wang, W., Lee, X., Xiao, W., Liu, S., Schultz, N., Wang, Y., ... & Zhao, L. (2018). Global lake evaporation accelerated by changes in surface energy allocation in a warmer climate. Nature Geoscience, 11(6), 410-414.

Wang, X., Shi, K., Zhang, Y., Qin, B., Zhang, Y., Wang, W., ... & Jeppesen, E. (2023). Climate change drives rapid warming and increasing heatwaves of lakes. Science Bulletin, 68(14), 1574-1584.

Wilcke, R. A. I., Kjellström, E., Lin, C., Matei, D., Moberg, A., & Tyrlis, E. (2020). The extremely warm summer of 2018 in Sweden–set in a historical context. Earth System Dynamics, 11(4), 1107-1121.

Wilhelm S. & Adrian, R. (2008). Impact of summer warming on the thermal characteristics of a polymictic lake and consequences for oxygen, nutrients and phytoplankton. Freshwater Biology, 53, 226-237.

Wilson, R. C., Hook, S. J., Schneider, P., Schladow, S. G. (2013). Skin and bulk temperature difference at Lake Tahoe: A case study on lake skin effect. Journal of Geophysical Research: Atmospheres, 118(18):10,332–10,346.

Woolway, R. I., Jennings, E., Shatwell, T., Golub, M., Pierson, D. C., & Maberly, S. C. (2021). Lake heatwaves under climate change. Nature, 589(7842), 402-407.

Woolway, R. I., Merchant, C. J., Van Den Hoek, J., Azorin-Molina, C., Nõges, P., Laas, A., ... & Jones, I. D. (2019). Northern hemisphere atmospheric stilling accelerates lake thermal responses to a warming world. Geophysical Research Letters, 46(21), 11983-11992.

Xiao, K., Griffis, T. J., Baker, J. M., Bolstad, P. V., Erickson, M. D., Lee, X., ... & Nieber, J. L. (2018). Evaporation from a temperate closed-basin lake and its impact on present, past, and future water level. Journal of Hydrology, 561, 59-75.

Yang, K., Lu, H., Yue, S., Zhang, G., Lei, Y., La, Z., & Wang, W. (2018). Quantifying recent precipitation change and predicting lake expansion in the Inner Tibetan Plateau. Climatic Change, 147, 149-163.

Yousefi, A. & Toffolon, M. (2022). Critical factors for the use of machine learning to predict lake surface water temperature. Journal of Hydrology, 606, p.127418. https://doi.org/10.1016/j.jhydrol.2021.127418

Yousefi (2023). Investigating the Crucial Factors Impacting the Accuracy of Machine Learning Models for Lake Surface Water Temperature and Ice Thickness Prediction, PhD Thesis, Deparment of Civil, Environmental and Mechanical Engineering, University of Trento.

Zhang, R., Sun, C., Zhu, J., Zhang, R., & Li, W. (2020). Increased European heat waves in recent decades in response to shrinking Arctic sea ice and Eurasian snow cover. NPJ Climate and Atmospheric Science, 3(1), 7.

Zhao, D., Huang, J., Li, Z., Yu, G., & Shen, H. (2023). Dynamic monitoring and analysis of chlorophyll-a concentrations in global lakes using Sentinel-2 images in Google Earth Engine. Science of The Total Environment, 169152.

Zhao, G., Li, Y., Zhou, L., & Gao, H. (2022). Evaporative water loss of 1.42 million global lakes. Nature Communications, 13(1), 3686.

Zhou, W., Wang, L., Li, D., & Leung, L. R. (2021). Spatial pattern of lake evaporation increases under global warming linked to regional hydroclimate change. Communications Earth & Environment, 2(1), 255.

Zhu, S., Ptak, M., Choiński, A., & Wu, S. (2020). Exploring and quantifying the impact of climate change on surface water temperature of a high mountain lake in Central Europe. Environmental monitoring and assessment, 192, 1-11.

Zhu, S., Ptak, M., Yaseen, Z. M., Dai, J., & Sivakumar, B. (2020). Forecasting surface water temperature in lakes: A comparison of approaches. Journal of Hydrology, 585, 124809.

Zhu, S., Ptak, M., Yaseen, Z. M., Dai, J., & Sivakumar, B. (2020b). Forecasting surface water temperature in lakes: A comparison of approaches. Journal of Hydrology, 585, 124809.